

Wetting and Penetration Behavior of Resin/Wood Interfaces

Christa Lauren Stables

Thesis submitted to the faculty of the Virginia Polytechnic Institute and State University in partial fulfillment of the requirements for the degree of

Master of Science

In

Forest Products

Charles E. Frazier, Chair

Maren Roman

Audrey Zink-Sharp

August 23, 2017

Blacksburg, Virginia

Keywords: Wetting, Penetration, Adhesives, Lucas-Washburn Equation,
Wood

Wetting and Penetration Behavior of Resin/Wood Interfaces

Christa Lauren Stables

ACADEMIC ABSTRACT

The goal of this project was improve the fundamental understanding of the wood-resin interaction, by looking at the relationship between the resin wetting onto wood and the resulting penetration into wood lumens. Wetting was analyzed with the sessile drop method, which observed the initial contact angle and change in contact angle over 35s. Penetration was measured within each individual tracheid. The Lucas-Washburn equation analyzed the wetting and penetration by calculating the penetration and comparing it to the measured penetration.

Wetting of four resins was compared on 3 species, to improve the understanding of adhesive wetting behavior. This study agreed with previous research, that the non-aqueous resin exhibited favorable wetting and presumably better penetration than aqueous resins, with exception of urea-formaldehyde.

Wetting and penetration of pMDI was studied on 5 wood species using the Lucas-Washburn equation. The wetting behaviors exhibited grain and species effects, which had implications on the resin availability for flake/strand-based composite products. The greater surface energy of loblolly pine most likely accounted for the significantly greater penetration of loblolly pine compared to Douglas-fir. The calculated penetration, via the Lucas-Washburn equation, exceeded the measured penetration, but it was concluded that the Lucas-Washburn equation predicted penetration reasonably well.

Wetting and penetration of phenol-formaldehyde and subsequent adhesives was compared on 3 wood species using the Lucas-Washburn equation. All contact angles were unfavorable due to a skin formation. The Lucas-Washburn equation did not predict any penetration; however, penetration was observed with all systems. The findings suggest that the system was too complex for the Lucas-Washburn equation to be able to predict accurately.

Wetting and Penetration Behavior of Resin/Wood Interfaces

Christa Lauren Stables

GENERAL ABSTRACT

Although the wood-based composites industry has been in operation for over a century, fundamental aspects of the wood/resin interaction- what happens when the liquid resin touches wood- remain poorly understood. An important aspect of this wood/resin interaction is penetration, which is critical to the strength and durability of wood-based composites. The two types of resins used, oil-based and water-based, were observed on a variety of wood species, Douglas-fir, loblolly pine, spotted gum, European beech and yellow-poplar. When using the oil-based resin, penetration measurements were in reasonable agreement with theoretical predictions. However, when using the water-based resins, the theory predicted no penetration which contradicted measurements- a shallow penetration was clearly observed. This means that parameters modeled by theory were in error, and this is sensible because we expect water to transfer from resin into the dry wood. Consequently, controlling parameters such as resin viscosity, resin surface tension, and wood surface energy were changing. This contributes fundamental knowledge, providing a better understanding of a critical step in the manufacture of wood-based composites, the materials most North Americans use to build their homes.

ACKNOWLEDGEMENTS

First and foremost, I would like to thank my Lord and Savior Jesus Christ, without His guidance on my life, I would not be where I am today. I am thankful He provided this opportunity for me to continue my education, and for giving me the strength and endurance I needed to succeed.

I would like to thank my major professor and committee chair, Dr. Charles Frazier. My first exposure to the wood composite industry was under his supervision as a summer undergraduate research student. His passion and knowledge of wood composites was influential in my decision to pursue a Master's degree.

I would also like to thank my committee members, Dr. Maren Roman and Dr. Audrey Zink-Sharp; their support and expertise was very beneficial to this work. I would like to thank the Wood-Based Composites Center for funding for this project, as well as Ms. Linda Caudill, Managing Director for the Wood-Based Composites Center. Her experience working in the wood composites industry was a valuable resource as I decided to continue my education, and now as I pursue a career in wood science. As my mentor for the past 6 years, I have learned several invaluable life-lessons from her, and I am thankful for our friendship.

I would also like to thank the entire faculty, staff, and students of the Department of Sustainable Biomaterials of whom I worked alongside with while pursuing both my Bachelor's and Master's degrees. Particularly, I would like to thank David Jones for his assistance with my project, and friendly discussions. I would also like to thank the graduate student research group that I worked with, Dr. Ann Norris, Dr. Guigui Wan, Mohammad Tasooji, Niloofar Yousefi-Shivyari, and Lourdes Orejuela. I thoroughly enjoyed all of our discoveries and conversations, both scientific and interpersonal. I would like to thank Ms. Debbie Garnand and Ms. Angie Riegel for their friendly conversations, and their help with shipping all of my specimens.

Last, and most importantly, I would like to thank my husband—John Stables for his continued love, support and countless hugs throughout this process, I would not have

made it through without him. I would also like to thank my parents—David and Karen Weaver, as well as my additional family—Ed, Donna, and Lara Stables, and friends, both near and distant; their encouragement and support have made this work possible.

Table of Contents

ACADEMIC ABSTRACT	iii
GENERAL ABSTRACT	iv
ACKNOWLEDGEMENTS	iii
1. Introduction and Literature Review	1
1.1 Introduction	1
1.2 Literature Review.....	2
1.3 Methods of penetration analysis	9
1.4 Application of the Lucas-Washburn equation.....	10
2. A wetting comparison of 4 common wood resins on 3 wood species	15
2.1 Introduction	15
2.2 Experimental.....	16
Materials	16
Resin viscosity.....	17
Resin surface tension	17
Wetting Measurements	17
Statistical Methods	18
2.3 Results and Discussion.....	18
Resin Properties	18
Wetting Behavior.....	19
Influence of resin type on wetting behavior	22
2.4 Summary	24
3. Applicability of the Lucas-Washburn Equation for predicting pMDI penetration	27
3.1 Introduction	27
3.2 Materials and Methods	28
Materials	28
Resin viscosity.....	29
Resin surface tension	29
Wetting Measurements	29
Penetration Measurements.....	30
Statistical Methods	30

3.3	Results and Discussion	31
	Wetting	31
	Grain orientation and pMDI wetting	33
	Species effects and pMDI wetting.....	37
	Penetration prediction via the Washburn equation.....	38
3.4	Summary	44
4.	Influence of surfactant and fillers/extenders on Phenol-formaldehyde resin wetting and penetration	48
4.1	Introduction	48
4.2	Materials and Methods	49
	Materials	49
	Resin viscosity.....	51
	Resin surface tension	51
	Wetting Measurements	51
	Penetration Measurements.....	52
	Statistical Methods	52
4.3	Results and Discussion	52
	Resin Properties	52
	Wetting	53
	Effects from the adhesives and wetting behavior	54
	Penetration prediction via the Washburn equation.....	55
	Meniscus Favorability	58
4.4	Summary	60
5.	Summary and Future Research	63
6.	APPENDICES	65
	A. Applicability of the Lucas-Washburn equation for predicting pMDI penetration .	65
	B. Influence of surfactant and fillers/extenders on Phenol-formaldehyde resin wetting and penetration.....	69
	C. Viscosity Flow Curve	75

List of Figures

Figure 1-1: Liquid contacting a solid surface; contact angle (θ) is indicated.....	2
Figure 1-2: Example image of droplet on wood specimen.	2
Figure 1-3: Pendant drop shape diagram.	4
Figure 1-4: On the left is the two monomers making up phenol-formalehyde, on the right is partial structure of cured phenol-formaldehyde resin.	6
Figure 1-5: On the left is the two monomers making up urea-formalehyde, on the right is partial structure of cured urea-formaldehyde resin.	7
Figure 1-6: On the left is the pMDI resin, on the right is partial structure of cured pMDI resin. ..	7
Figure 1-7: Illustration of the orthotropic nature of wood (Walinder, 2000).	8
Figure 2-1: Example wetting curves of all resins on loblolly pine cross-sectional surfaces, earlywood. (n = 10-12)	20
Figure 2-2: Example wetting curves of all resins on Douglas-fir cross-sectional surfaces, earlywood. (n = 10-13)	21
Figure 2-3: Example wetting curves of all resins on spotted gum cross-sectional surfaces, earlywood. (n = 8-14)	21
Figure 2-4: Example variation of PF OSB wetting on Douglas-fir cross-sectional surfaces, earlywood (n = 10).....	21
Figure 2-5: Initial contact angle of all resins as a function of species. Statistical significance shown by capital letters, but only within each species. (n = 8-14).....	22
Figure 2-6: Percent change in contact angle of all resins as a function of species. Statistical significance shown by capital letters, but only within each species. (n = 8-14).....	23
Figure 3-1: Example wetting curves of pMDI on the cross-sectional surface of all five species. (n = 10-14).....	32
Figure 3-2: Example wetting curves of pMDI on the tangential surface of all five species. (n = 10)	32
Figure 3-3: Example wetting curves of pMDI on the radial surface of all five species. (n = 10)	33
Figure 3-4: Example variation of pMDI wetting on the tangential surface of yellow-poplar (n =10).....	33

Figure 3-5: pMDI initial contact angles as a function of grain and species. Statistical significance shown by capital letters, but only within each species. (n = 10-14)	34
Figure 3-6: Percent change in pMDI contact angles as a function of species and grain. Statistical significance shown by capital letters, but only within each species. (n = 10-14).....	36
Figure 3-7: Initial contact angle of pMDI as a function of species and grain orientation. Statistical significance shown by capital letters, but only within each surface type. (n = 10-14)	37
Figure 3-8: Percent change in pMDI contact angles as a function of species and grain orientation. Statistical significance shown by capital letters, but only within each surface type. (n = 10-14)	38
Figure 3-9: Example wetting curves of pMDI on Douglas-fir and loblolly pine. (n = 10)	39
Figure 3-10: Boxplots comparing the calculated and measured penetration of pMDI resin into loblolly pine and Douglas-fir cross-sectional surfaces. Statistical significance shown by capital letters. (Whiskers: 5 th & 95 th percentile; open box: 25 th & 75 th percentile; line: median; closed square: mean) (n =18-48 cells per slide with n = 10 slides per species).....	40
Figure 3-11: Correlation of specific penetration vs lumen diameter on loblolly pine earlywood (R ² = 0.85); each color represents one section (n = 10).....	42
Figure 3-12: Calculated contact angle vs measured penetration on loblolly pine. (n=10)	43
Figure 3-13: Box plot comparing the predicted contact angles of Douglas-fir and loblolly pine. (Closed triangles: min and max; whiskers: 5 th & 95 th percentile; open box: 25 th & 75 th percentile; line: median; closed square: mean) (n =18-48 cells per slide with n = 10 slides per species)	44
Figure 4-1: Example wetting of all adhesives studied on loblolly pine cross-sectional surfaces; note scale. (n = 10-11)	54
Figure 4-2: Initial contact angles of all adhesives as a function of species. Statistical significance shown by p-values, but only within each species. (n = 8-13).....	54
Figure 4-3: Percent change in contact angles of all adhesives as a function of species. Statistical significance shown by capital letters, but only within each species. (n = 8-13).....	55
Figure 4-4: Specific penetration of all adhesives as a function of species. Statistical significance shown by capital letters, but only within each species. (n =13-66 cells per slide with n = 9-10 slides per species)	56

Figure 4-5: Specific penetration of all species as a function of adhesive type. Statistical significance shown by capital letters, but only within each adhesive type. (n =13-66 cells per slide with n = 9-10 slides per species) 58

Figure 4-6: Diagrams showing the expected menisci under favorable and unfavorable wetting. 59

Figure 4-7: Average meniscus favorability of all adhesives as a function of species. Statistical significance shown by capital letters, but only within each species. (n =13-71 cells per slide with n = 9-10 slides per species)..... 59

Figure 6-1: Correlation of specific penetration vs lumen diameter on Douglas-fir ($R^2 = 0.85$). (n =10)..... 65

Figure 6-2: Example penetration of pMDI on loblolly pine; 5X (n =31-48 cells per slide with n = 10 slides) 66

Figure 6-3: Example penetration of pMDI on Douglas-fir; 5X (n =18-39 cells per slide with n = 10 slides) 67

Figure 6-4: Calculated contact angle vs measured penetration on Douglas-fir. (n =10) 68

Figure 6-5: Example wetting curves of all adhesives on Douglas-fir cross-sectional surface, earlywood; note scale. (n = 9-13) 69

Figure 6-6: Example wetting curves of all adhesives on spotted gum cross-sectional surface; note scale. (n = 8-10) 69

Figure 6-7: Example penetration of PLY RESIN on loblolly pine; 5X (n =13-29 cells per slide with n = 10 slides)..... 70

Figure 6-8: Example penetration of PLY RESIN on loblolly pine; 5X (n =13-29 cells per slide with n = 10 slides)..... 70

Figure 6-9: Example penetration of PLY RESIN on loblolly pine; 5X (n =13-29 cells per slide with n = 10 slides)..... 71

Figure 6-10: Example penetration of PLY FORM on Douglas-fir; 5X (n =16-24 cells per slide with n = 9 slides)..... 71

Figure 6-11: Example penetration of PLY FORM on Douglas-fir; 5X (n =16-24 cells per slide with n = 9 slides)..... 72

Figure 6-12: Example penetration of PLY FORM on Douglas-fir; 5X (n =16-24 cells per slide with n = 9 slides)..... 72

Figure 6-13: Example penetration of PLY SURF 0.5% on spotted gum; 10X (n =19-66 cells per slide with n = 10 slides) 73

Figure 6-14: Example penetration of PLY SURF 0.5% on spotted gum; 10X (n =19-66 cells per slide with n = 10 slides) 73

Figure 6-15: Example penetration of PLY SURF 0.5% on spotted gum; 10X (n =19-66 cells per slide with n = 10 slides) 74

Figure 6-16: Viscosity steady-state flow curves (concentric cylinder; 0.5 to 3000 **1s**; 25 °C) (n = 5-14)..... 75

List of Tables

Table 2-1: Liquid properties of the four resins studied; average (stdev).....	18
Table 3-1: Pair-wise comparison of Douglas-fir earlywood and latewood wetting. (n = 10)	36
Table 4-1: Phenol-formaldehyde formulation in mass fraction.....	50
Table 4-2: Liquid properties of the four adhesives studied; average (stdev).....	53

1. Introduction and Literature Review

1.1 Introduction

When wood adhesives contact (or wet) the wood surface, intermolecular forces promote or inhibit penetration of the adhesive into the porous wood structure. Subsequently, adhesive cure (solidification) produces a bond in which the cured adhesive exhibits a complex three-dimensional configuration that reflects the wood surface and its subsurface cellular anatomy (Paris & Kamke, 2015). The strength of bonding (from secondary and perhaps primary forces) and the distribution of stresses in and around the bond ultimately dictate the performance of wood-based composites. Since these products are the preferred home-building materials of most North Americans, the wetting and penetration behavior of wood adhesives holds great practical significance. However, the wood-based composites industry has over 100 years of operation (Barbu et al., 2014; Maloney, 1996), so one naturally wonders why wood/adhesive wetting and penetration behavior merits study today. Regardless of the industry, however mature, there is an endless drive for improvement, mostly due to economic competition and sometimes government regulation. Due to the fierce economic competition, it is safe to say that the easily accessible information has been surpassed and that industrial advances are increasingly dependent upon challenging scientific inquiries and technologies. If wood adhesives were pure liquids, and if wood was a simple porous solid, like fritted glass for example, then wood/adhesive wetting and penetration would be easy to model and manipulate. Wood adhesives are rarely if ever pure liquids, and solid wood is a highly complex and variable, porous solid. In other words, while wood/adhesive wetting and penetration is central to the manufacture and performance of wood-based composites, this fundamental relationship is poorly understood. The goal of this research was to improve the understanding between adhesive wetting onto wood, and the subsequent penetration into wood. This work only considers penetration due to capillary forces, the events prior to bond consolidation and compaction.

1.2 Literature Review

When a pure liquid wets (contacts) a clean, non-porous surface, the quality of wetting is observed through the angle of contact, depicted in Figure 1. When the contact angle is less than 90° , the quality of wetting is often referred to as “favorable.” Likewise, unfavorable wetting is said to occur when the contact angle exceeds 90° .

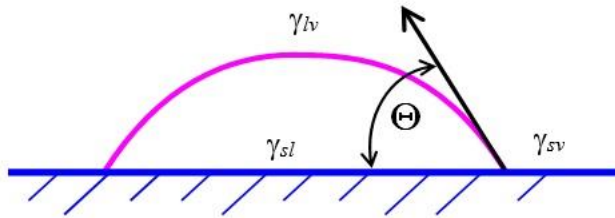


Figure 1-1: Liquid contacting a solid surface; contact angle (θ) is indicated.

There are three common ways to measure the contact angle, sessile drop, Wilhelmy slide and advancing/receding contact angle (Berg, 2010). For this study, the contact angle measurements were based off of the sessile drop method, where the liquid was dispensed on the solid surface through a syringe. A high-speed camera was used to view the droplet horizontally from the side and capture images, shown in Figure 1-2. The droplet was then analyzed by the computer software, First Ten Angstroms 32 (FTA 32). Since wood, a porous surface, was used, the contact angle should continuously decrease over time, due to liquid penetration into capillaries (Berg, 2010).

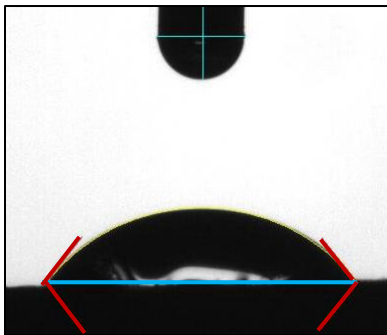


Figure 1-2: Example image of droplet on wood specimen.

The Young equation (1-1), is commonly used to analyze the contact angle. This equation associates the solid surface energy (solid/vapor interface), γ_{sv} , the liquid/solid interfacial energy (liquid/solid interface), γ_{sl} , and the liquid surface tension (liquid/vapor interface), γ_{lv} , to the resulting contact angle, θ , (the minimization of the system free energy) (Berg, 2010); see Figure 1-1 for illustration.

$$\gamma_{sv} = \gamma_{sl} + \gamma_{lv} \cos \theta \quad (1-1)$$

Solid surface energy is the result of higher energy molecules at the surface compared to the lower energy bulk molecules of a solid (hereafter referred to as surface energy). Surface energy is unmeasurable but can be estimated from the Young equation. Liquid surface tension is the result of the intermolecular forces minimizing the liquid surface area (hereafter referred to as surface tension). Surface tension is measurable by multiple methods, such as capillary rise, Wilhelmy plate, Du Nouy ring, drop shape and drop weight (Berg, 2010). In this research the drop shape and drop weight methods were used according to the techniques of Yang and Frazier (2016).

To measure surface tension via the drop shape method, the liquid was dispensed at a steady rate into a pendant drop shape (Figure 1-3). An image was captured of the droplet just before detachment, which the FTA 32 software applied to the Young-Laplace equation (Equation 1-2). The Young-Laplace equation relates the surface tension, γ , to the density difference between the liquid and vapor, $\Delta\rho$, the curvature at the droplet apex, R_o , the gravitational constant, g , and the shape factor, β . The shape factor accounts for the fact that the droplet formation was from the surface tension and the gravitational forces (Woodward).

$$\gamma = \frac{\Delta\rho R_o g}{\beta} \quad (1-2)$$

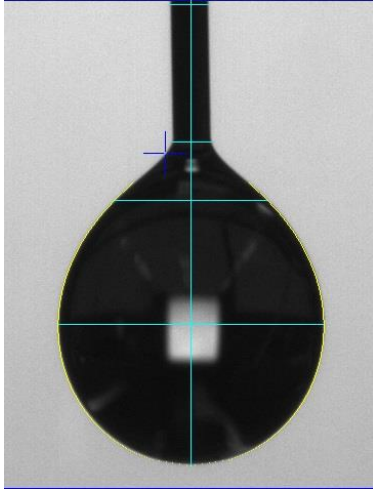


Figure 1-3: Pendant drop shape diagram.

The drop weight method was accomplished by applying the average droplet mass from the drop shape method to Tate's law (Tate, 1864). A small amount of liquid will always remain on the needle tip after the droplet detaches. Therefore, the Harkins-Brown (HB) correction factor was applied, transforming Tate's Law into Equation 1-3 (Lando & Oakley, 1967). The liquid surface tension, γ , was related to the droplet mass, m , the gravitational constant, g , the HB correction factor, F , and the tip radius, R .

$$\gamma = \frac{mgF}{R} \quad (1-3)$$

As previously mentioned, the relationship between wetting and penetration is complicated and not thoroughly understood; one in which the liquid properties must relate to capillary flow. The Lucas-Washburn equation, Equation 1-4, takes into account the capillary radius, r , liquid viscosity, η , surface tension, γ , contact angle, θ , and total time, t , to predict the penetration depth of the liquid, h , (Lucas, 1918; Washburn, 1921). This equation originally measured the capillary action of simple liquids with single capillaries, which only adsorbed through capillary action. In the following research, the Lucas-Washburn equation was applied to wood, which would be more complex, assuming non-uniform capillaries as well as absorption into the capillary wall.

$$h^2 = \frac{r\gamma \cos \theta}{2\eta} t \quad (1-4)$$

Time, t , is referred to as the wetting period. This was the time from initial contact of the resin onto the specimen, through wetting, until the resin was cured, including specimen transport time to the method of cure. This time was not fixed since it was a parameter of the Washburn equation.

Wetting is typically based on factors such as viscosity, surface tension, and surface energy (Berg, 2010). In wood adhesives, there are two main categories, aqueous and non-aqueous, which exhibit very different resin properties. As penetration occurs, the viscosity, η , of an aqueous resin increases rapidly due to the absorption of water from the resin into the cell walls (de Meijer, Thurich, et al., 2001; de Meijer, van de Velde, et al., 2001; Scheikl & Dunky, 1998). However, the exact rate of increase between viscosity and penetration is unknown (Paris & Kamke, 2015). It has been proposed that non-aqueous resins, such as pMDI, could penetrate into the cell wall microvoids, allowing for minor swelling in the cell wall (Frazier, 2003; Zheng et al., 2004). High molecular weight resins generally have higher viscosities, which have been proven to have greater dry out at the surface. Therefore they should exhibit less penetration than lower molecular weight resins (Kamke & Lee, 2007; Marra, 1992).

Favorable wetting occurs when the contact angle, θ , is less than 90° and indicates that capillary uptake is happening (Scheikl & Dunky, 1998; Shi & Gardner, 2001). A contact angle greater than 90° is considered unfavorable and no penetration would be expected to occur. However, the contact angle can change over time, and a significant decrease in contact angle indicates favorable wetting and penetration (Berg, 2010). From Equation 1-1, we see that favorable wetting occurs with a lower surface tension and higher surface energy. Since lower surface tensions are typical of non-aqueous resins, favorable wetting was expected to occur. Surfactants are known to decrease the surface tension of the liquid (de Meijer, van de Velde, et al., 2001), and are used in industrial practice for curtain coating application.

The wood composites industry uses resins, which are typically viscous liquids that can be either aqueous or non-aqueous. Many resins in the wood composites industry are aqueous, where the curing process occurs from polymerization and water loss. Phenol-formaldehyde (PF) and urea-formaldehyde (UF) are two commonly used water based resins used in the research below. PF is known for its durability, strength and water-resistance once cured; an example of PF monomer

and partially cured resin is shown in Figure 1-4. Typically used for laminate and strand/flake based applications, PF stays on the surface of the wood leaving resin available for adhesion to occur. PF is more alkaline in nature (pH: 8-10) with a higher surface tension of 69 mJ/m² (Yang & Frazier, 2016). Aqueous resins that have substances added, such as surfactants, fillers and extenders, are known as adhesives. Surfactants are commonly added for the industrial practice of curtain coating applications. Fillers, such as alder bark, walnut shell or corn cob residue, are added to modify the resin and help lower the overall cost of the adhesive (Yang, 2014). Extenders, such as wheat flour, are added to aid in the adhesive properties (Yang, 2014).

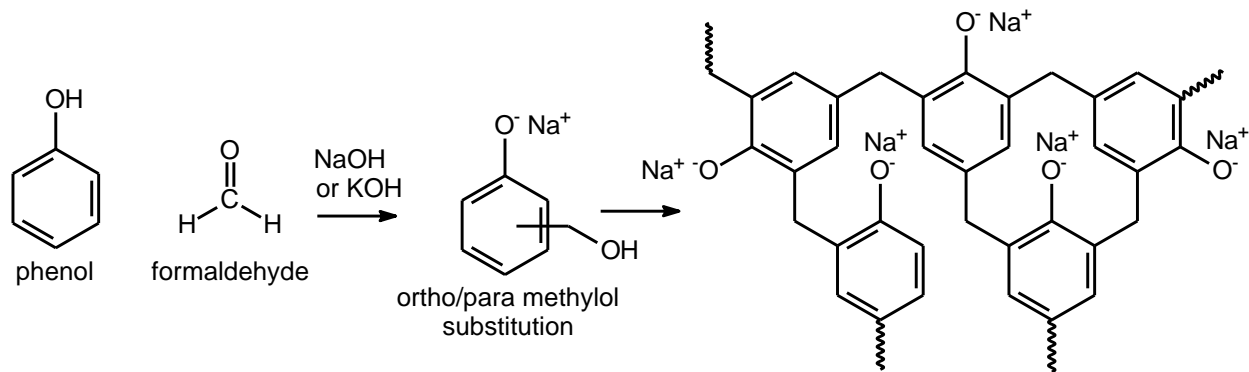


Figure 1-4: On the left is the two monomers making up phenol-formaldehyde, on the right is partial structure of cured phenol-formaldehyde resin.

UF is known for its clear bondline and rapid cure. UF wetting was found to have more spreading and a greater decrease in volume compared to PF (Lee et al., 2007). UF typically has an acid catalyst added, making it more acidic and increasing the molecular weight as curing (pH: 5-8) (Conner, 1996; Scheikl & Dunky, 1998). Typically only used with particleboard and strand based products, also having a higher surface tension of 56 mJ/m² (Liu et al., 2004).

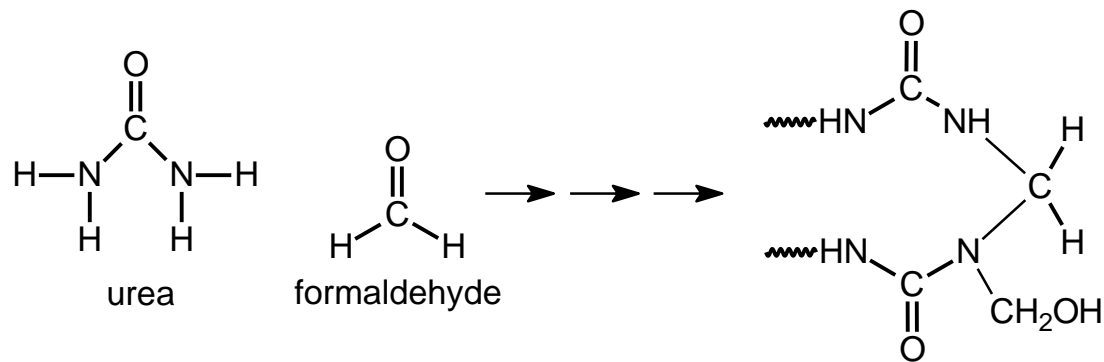


Figure 1-5: On the left is the two monomers making up urea-formaldehyde, on the right is partial structure of cured urea-formaldehyde resin.

A common non-aqueous resin used in the research below is polymeric methylene diphenyl diisocyanate (pMDI), which is known to wet rapidly and is highly reactive with water. The rapid wetting of pMDI is attributed to its low surface tension of 46 mJ/m² (Liu et al., 2004), and is known to penetrate deeply, not leaving much resin on the surface for adhesion. However pMDI does have adequate adhesion with strand/flake applications. Of all the industrial resins, pMDI is most like a pure liquid, only having isocyanate monomer and oligomers (DP <12) (Frazier, 2003). The isocyanate bond will also cure instantaneously with a primary amine present, such as the NH₃ used in the research below.

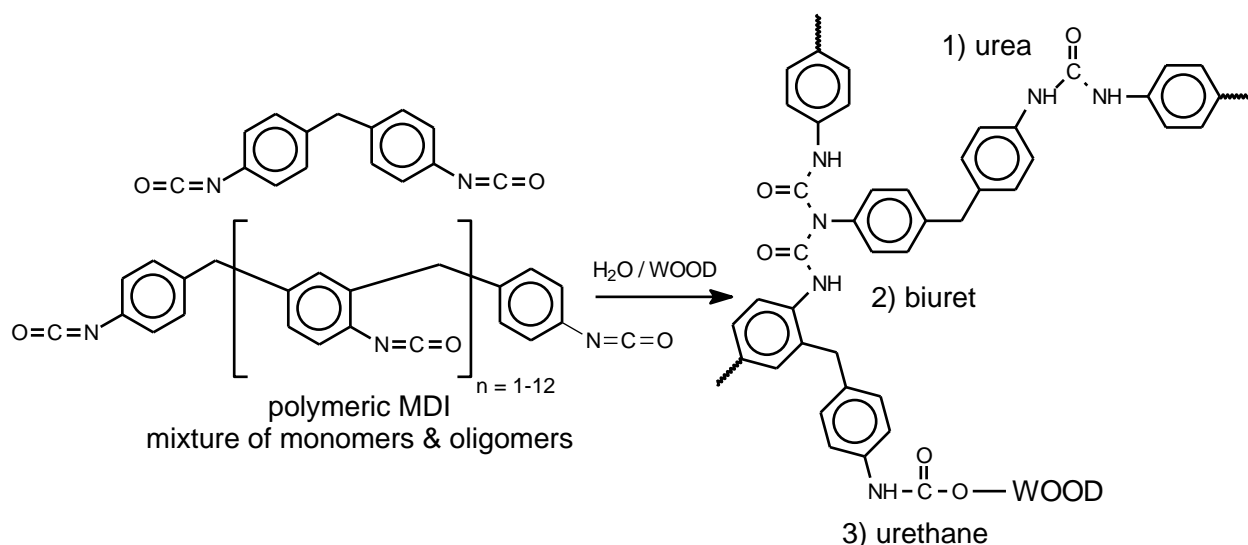


Figure 1-6: On the left is the pMDI resin, on the right is partial structure of cured pMDI resin.

Wetting and penetration is also affected by surface energy, which is altered by surface preparation and wood cellular anatomy (Gardner et al., 1991; Mirabile, 2015). In this study, the surfaces were microtomed to obtain a smooth surface for contact angle analysis. This increased the surface energy, however, since all of the surfaces were microtomed in the same fashion, this effect was not taken into account. Wood moisture content is another contributing factor in surface energy, in that higher moisture content increases wettability. However, moisture content was found to not be as influential as surface roughness or grain orientation (Scheikl & Dunky, 1998); it was controlled in the research discussed below.

Wood is an orthotropic material, meaning it has three perpendicular axes with different properties on each, shown in Figure 1-3. The cross-section, or end-grain, is where the lumen openings are located, allowing the quickest access for resin to penetrate into the cells; thus the contact angle should rapidly decrease, indicating lumen penetration (Scheikl & Dunky, 1998). Radial and tangential surfaces, if cut perfect, they would not have any open lumens for the resin to penetrate, which would only allow for the minimal cell wall penetration. Contact angles have been found to wet favorably along the side grain, as a result of spreading along the surface due to the longitudinal tracheids (de Meijer et al., 2000; Shi & Gardner, 2001). The difference in wetting between the end grain and side grain is due to the lower surface roughness on the side grain, producing better wettability. Wetting was observed on all three axes, but penetration was only on the end grain.

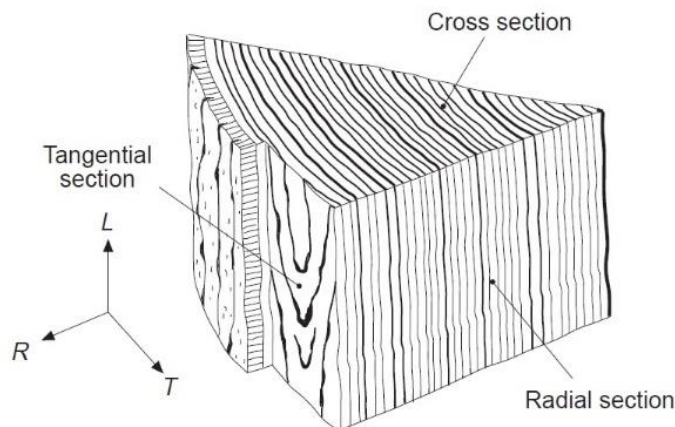


Figure 1-7: Illustration of the orthotropic nature of wood (Walinder, 2000).

Penetration into a wood cell lumen is defined as gross penetration and cell wall penetration. Gross penetration is the movement of liquid through the larger diameter cells, whereas cell wall penetration is the movement through the micro voids within the cell wall itself (Johnson & Kamke, 1992; Kamke & Lee, 2007). This study will look at aspects of both categories in adhesive/wood penetration.

For softwoods, most of the gross penetration is through the longitudinal tracheids and rays. Hardwood gross penetration mostly occurs through the vessels and the longitudinal fibers (Gavrilović-Grmuša et al., 2010; Kamke & Lee, 2007). Mirabile measured the surface energies of two softwoods used in this study, loblolly pine (*Pinus taeda*) and Douglas-fir (*Pseudotsuga menziesii*) (2017). Using an acid/base surface model by means of wetting with pure liquids, Mirabile found that loblolly pine had a 39% greater surface energy than Douglas-fir, indicating loblolly pine should have more favorable wetting. One of the hardwoods studied, spotted gum, (*Corymbia citriodora*) is known for tyloses present in the vessels and for a large number of extractives (Burch, 2015), both of which cause unfavorable wetting and penetration. Tyloses are present in some hardwoods. They are bubble-like structures within the vessel elements, typically known to limit penetration (Hoadley, 2000).

1.3 Methods of penetration analysis

Penetration can be viewed by multiple techniques: light microscopy, fluorescence microscopy, scanning electron microscopy (SEM), transmission electron microscopy (TEM), and micro X-ray tomography (XT). Optical methods were used in this study and provide color contrast and filters which can be useful to identify the resin from the wood. However, the optical methods typically require water soaking which can alter the penetration if the cured resin is water soluble (Kamke & Lee, 2007).

Resin penetration into wood can be quantified in many ways: specific penetration, maximum penetration, effective penetration, weighted penetration and average penetration depth (Gavrilović-Grmuša et al., 2010; Johnson & Kamke, 1992; Paris & Kamke, 2015). Specific penetration, Equation 1-5, was used in this study and is the average of the depth of penetration of each cell, c_i , measured from the bondline (Gavrilović-Grmuša et al., 2010). The measurements

were taken on a microtomed section placed on a glass slide, and the total width of penetration in all the capillaries, or lumens, was seen within one section.

$$SP = \frac{\sum_1^n c_i}{n} \quad (1-5)$$

1.4 Application of the Lucas-Washburn equation

Since the Washburn equation is used to estimate penetration, the goal of this research was to validate this claim using wood. The rest of this chapter is devoted to previous studies that compared wetting and penetration, including those that applied the Washburn equation.

Scheikl and Dunky studied earlywood and latewood wetting using four different species with a urea formaldehyde resin (1998). They compared the initial contact angle and the change in contact angle, and found that earlywood had better wetting than latewood. The greater change in contact angle indicates favorable penetration, thus it was estimated that earlywood should have greater penetration than latewood.

Shi and Gardner compared two resins used in this study, phenol-formaldehyde and pMDI, on two species used in this study, Douglas-fir and loblolly pine (2001). They generated a wetting model that supplied a K-value, which increased based on the contact angle change over time. Since the greater change indicates favorable wetting, a greater K-value indicates favorable wetting. The goal was to use the K-value to estimate the penetration. However, Shi and Gardner did not measure penetration, instead they presumed an understanding of penetration based on the K-value. When comparing the resins, pMDI exhibited significantly better wetting and presumably better penetration compared to the phenol-formaldehyde. Douglas-fir exhibited a less favorable wetting compared to southern pine.

After studying the wetting behavior of aqueous and non-aqueous coatings, de Meijer, Thurich et al. (2001), described three cases to portray wetting. 1) stable droplet diameter and height with minimal contact angle and volume change 2) stable droplet diameter with a height, contact angle and volume decrease; attributed to lumen penetration 3) droplet diameter, height and contact angle decrease; attributed to both wetting and lumen penetration. The third case indicates a significant change in contact angles and demonstrates the most favorable wetting.

When aqueous and non-aqueous coatings were applied to the Washburn equation, the predicted penetration was significantly greater compared to the measured penetration for aqueous coatings; indicating that the viscosity rapidly increased, decreasing the penetration (de Meijer, Thurich, et al., 2001; de Meijer, van de Velde, et al., 2001). It was also found that the Washburn equation did not accurately predict the penetration of the non-aqueous coatings. Higher surface tensions, higher viscosity and an increase in surfactant were found to decrease capillary penetration. A theory was suggested that at the penetration front, more water was absorbed, which increased the viscosity at the front and greatly inhibited penetration.

Lastly, using a computer model, the Washburn equation was applied to bamboo. The equation predictions were found to not be as accurate if the cell lumens had lower moisture content (Li et al., 2014). It was also found that phenol-formaldehyde (PF) with variable ratios of polyvinyl acetate (PVAC), absorbed roughly along the time scale that the Washburn equation predicted.

There are many peculiar issues when comparing wetting and penetration on wood. Wood is a complicated surface, making resin penetration into wood difficult to predict. This research will measure all of the parameters of the Washburn equation and compare the measured penetration to the actual penetration.

References

- Barbu, M. J., Reh, R., & Irle, M. (2014). Wood-Based Composites. In A. D. Aguilera, J. Paulo (Ed.), *Research Developments in Wood Engineering and Technology* (pp. 1-45). Hershey, PA: Engineering Science Reference (an imprint of IGI Global).
- Berg, J. C. (2010). *An Introduction to Interfaces and Colloids: The Bridge to Nanoscience*. Tuck Link, Singapore: World Scientific Publishing Co. Pte. Ltd.
- Burch, C. (2015). *Adhesion Fundamentals of Spotted Gum (Corymbia citriodora)*. (Masters of Science Master's of Science), Virginia Tech, Blacksburg, VA.
- Conner, A. H. (1996). Urea-formaldehyde adhesive resins. 8497-8501.
- de Meijer, M., Haemers, S., Cobben, W., & Militz, H. (2000). Surface energy determinations of woods: Comparison of Methods and wood species. *Langmuir*, 16, 9352-9359.

- de Meijer, M., Thurich, K., & Militz, H. (2001). Quantitative measurements of capillary coating penetration in relation to wood and coating properties. *Holz als Roh- und Werkstoff*, 59, 35-45.
- de Meijer, M., van de Velde, B., & Militz, H. (2001). Rheological Approach to the capillary penetration of coating into wood. *Journal of Coatings Technology*, 73(914), 39-51.
- Frazier, C. E. (2003). Isocyanate Wood Binders. In A. M. Pizzi, K. L. (Ed.), *Handbook of Adhesive Technology, Revised and Expanded* (Vol. 2, pp. 681-694). New York, NY: Marcel Dekker Inc.
- Gardner, D. J., Generalla, N. C., Gunnells, D. W., & Wolcott, M. P. (1991). Dynamic Wettability of wood. *Langmuir*, 7, 2498-2502.
- Gavrilović-Grmuša, I., Dunky, M., Miljković, J., & Djiporović-Momčilović, M. (2010). Radial Penetration of Urea-Formaldehyde Adhesive Resins into Beech (*Fagus Moesiaca*). *Journal of Adhesion Science and Technology*, 24(8-10), 1753-1768. doi:10.1163/016942410x507812
- Hoadley, R. B. (2000). *Understanding Wood: A Craftmans Guide to Wood Technology*. Newton, CT: The Taunton Press.
- Johnson, S. E., & Kamke, F. A. (1992). Quantitative Analysis of Gross Adhesive Penetration in Wood Using Fluorescence Microscopy. *The Journal of Adhesion*, 40(1), 47-61.
doi:10.1080/00218469208030470
- Kamke, F. A., & Lee, J. N. (2007). Adhesive Penetration in wood- A Review. *Wood and Fiber Science*, 39(2), 205-220.
- Lando, J. L., & Oakley, H. T. (1967). Tabulated correction factors for the drop-weight-volume determination of surface and interfacial tensions. *Journal of Colloid and Interfacial Science*, 25, 526-530.
- Lee, S., Shupe, T. F., & Hse, C. Y. (2007). Wetting behavours of phenol- and urea- formaldehyde resins as compatibilizers. *Wood and Fiber Science*, 39(3), 482-492.
- Li, H., Chen, F., Cheng, H., Deng, J., Wang, G., & Sun, F. (2014). Large-span Bamboo Fiber-based Composites, Part 1: A prediction model based on the Lucas-Washburn equation describing

the resin content of bamboo fiber impregnation with different PVAC/PF concentrations. *BioResources*, 9(4), 6408-6419.

Liu, Z.-M., Wang, F.-H., & Wang, X.-M. (2004). Surface structure and dynamic adhesive wettability of wheat straw. *Wood and Fiber Science*, 32(2), 239-249.

Lucas, R. (1918). Ueber das Zeitgesetz des kapillaren Aufstiegs von Flüssigkeiten. *Kolloid-Zeitschrift*, 23, 15-22.

Maloney, T. M. (1996). The family of wood composite materials. *Forest Products Journal*, 46(2), 19-26.

Marra, A. A. (1992). *Technology of Wood Bonding Principles in Practice*. New York, NY: Van Nostrand Reinhold.

Mirabile, K. (2015). *Investigating Differences between Douglas-fir and Southern Yellow Pine Bonding Properties*. (Master of Science), Virginia Tech, Blacksburg, VA.

Mirabile, K. V., & Zink-Sharp, A. (2017). Fundamental bonding properties of Douglas-fir and southern yellow pine wood. *Forest Products Journal*, In-Press. doi:<https://doi.org/10.13073/FPJ-D-17-00019>

Paris, J. L., & Kamke, F. A. (2015). Quantitative wood-adhesive penetration with X-ray computed tomography. *International Journal of Adhesion and Adhesives*, 61, 71-80.

Scheickl, M., & Dunky, M. (1998). Measurement of Dynamic and Static Contact Angles on Wood for the determination of its Surface Tension and the Penetration of Liquids into the wood Surface. *Holzforschung*, 52(1), 89-94.

Shi, S. Q., & Gardner, D., J. (2001). Dynamic adhesive wettability of wood. *Wood and Fiber Science*, 33(1), 58-68.

Tate, T. (1864). On the magnitude of a drop of liquid formed under different circumstances. *The London, Edinburgh, and Dublin Philosophical Magazine and Journal of Science*, 27, 176-180.

Walinder, M. (2000). *Wetting phenomena on wood: Factors influencing measurements of wood wettability*. KTH-Royal Institute of Technology, Stockholm.

Washburn, E. W. (1921). The Dynamics of Capillary Flow. *Physical Review*, 17(3), 273-283.
doi:10.1103/PhysRev.17.273

Woodward, R. P. Surface Tension Measurements Using the Drop Shape Method. In F. T. Angstroms (Ed.).

Yang, X. (2014). Organic fillers in phenol formaldehyde wood-adhesives. (Doctor of Philosophy), Virginia Tech, Blacksburg, VA.

Yang, X., & Frazier, C. (2016). Influence of organic fillers of surface tension of phenol-formaldehyde adhesives. *International Journal of Adhesion and Adhesives*, 66, 160-166.

Zheng, J., Fox, S. C., & Frazier, C. E. (2004). Rheological, wood penetration, and fracture performance studies of PF/pMDI hybrid resins. *Forest Products Journal*, 51(10), 74-81.

2. A wetting comparison of 4 common wood resins on 3 wood species

Abstract:

Wood-based composites such as plywood and oriented strand board (OSB) are commonly used for home manufacturing, therefore the bond performance between the resin and wood is critical. Wetting is often used to determine adhesive compatibility for wood-based composites. To give a more conclusive understanding of adhesive wetting, this research compared the wetting behaviors of four resins on three wood species. Contact angles were viewed by the sessile drop method, and analyzed by the initial contact angle and contact angle change over 35 seconds. pMDI exhibited favorable wetting and PF exhibited unfavorable wetting, as anticipated. However, urea-formaldehyde exhibited favorable wetting, which was unexpected and possibly due to the acid catalyst. Implications from this study coincide with previous research, that the non-aqueous resin exhibited favorable wetting and presumably better penetration than the aqueous resins, with exception of urea-formaldehyde. Future research was suggested with urea-formaldehyde wetting and penetration.

Keywords: Wetting, contact angle, wood adhesives, wood-based composites

2.1 Introduction

The performance of the wood-adhesive bond correlates strongly to resin wetting and penetration. Wetting can be evaluated by observing the wood/resin contact angle. Although sometimes misrepresentative of wood/resin wetting, the initial contact angle can indicate wood surface energy; whereas the dynamic or time dependent contact angle indicates favorable molecular interactions and penetration (Gavrilović-Grmuša et al., 2010; Sernek et al., 2004). Even though wood-based composites have been produced for over 100 years (Barbu et al., 2014; Maloney, 1996), the wood/resin interactions are so complex that many of the fundamental details of this interaction are poorly understood.

Wetting is affected by liquid surface tension and solid surface energy (Berg, 2010). It is commonly defined as either favorable or unfavorable if the contact angle is respectively less than

or greater than 90°. Correspondingly, for porous substrates like wood, the Young-Laplace relationship predicts that capillary uptake occurs when wetting is favorable; but not so when wetting is unfavorable (Berg, 2010). However, the Young-Laplace relationship does not account for liquid viscosity, a practical matter that is accounted for in the Lucas-Washburn equation (Lucas, 1918; Washburn, 1921), Equation 2-1, where the penetration distance, h , is related to the capillary radius, r , liquid surface tension, γ , liquid viscosity, η , cosine of the contact angle θ , and time, t .

$$h^2 = \frac{r\gamma \cos \theta}{2\eta} t \quad (2-1)$$

Analysis of the wetting process can be incredibly useful in determining the compatibility between resins and wood (Kamke & Lee, 2007). Wood species vary in surface energy and pore size, and resins vary in solids content, molecular weight distribution and properties. Therefore, it is important to understand the wetting behavior, in order to make a successful wood composite (Johnson & Kamke, 1992; Kamke & Lee, 2007). The effort described here analyzes the wetting behaviors, between commonly used industrial resins and wood species, to improve the understanding of resin wetting onto wood, and apply this insight to the wood-resin bond.

2.2 Experimental

Materials

Two liquid phenol-formaldehyde resins, 14B346, a plywood resin (PF PLY), and Solution D3, an oriented strand board resin (PF OSB), and a liquid urea-formaldehyde (UF) hardwood plywood resin, E4 and an ammonium sulfate catalyst were obtained from Arclin Specialty Chemicals Inc. Approximately two weight percent of the catalyst was added to the UF resin just prior to measurement. Polymeric (methylene diphenyl diisocyanate) (pMDI) Rubinate M[®], was obtained from Huntsman Polyurethanes. Three different wood species were obtained in the form of air-dried lumber: loblolly pine (*Pinus taeda*) from Critz, Virginia, USA; Douglas-fir (*Pseudotsuga menziesii*) from Benton, Oregon, USA; and spotted gum (*Corymbia citriodora*) from Queensland, Australia. Specimens were rough-cut into ~9 mm³ cubes, saturated in distilled water, and then microtomed (GSL1 sliding microtome) on the cross-sectional surface. The

specimens were dried by cycling between vacuum (0.15 mmHg) and dry N₂ three times and then stored with dry N₂/molecular sieves. The specimens were equilibrated to ~6% moisture content in a desiccator over a saturated magnesium chloride solution.

Resin viscosity

A TA Instruments AR G2 Rheometer was used (concentric cylinder geometry, diameter = 30.35 mm and gap = 1 mm) to obtain steady-state flow curves (25°C; 0.5 to 3000 s⁻¹; ramping up in shear, then ramping down with no delay between ramps; steady-state criteria = 3 consecutive data points collected in 1 minute or less, shear stress ≤ 5% change).

Resin surface tension

Resin density was measured using a 10 mL graduated cylinder. Approximately one milliliter increments were added using a syringe and the density was obtained from the linear slope of the mass/volume plot; the corresponding correlation coefficients (R²) were always above 0.99.

Surface tension was measured by the drop shape and drop weight methods at room temperature with a First Ten Angstroms, FTA 200, as described by Yang and Frazier (2016). The surface tensions reported below were from 10 trials analyzed separately using the drop shape and drop weight methods. The separate surface tensions were found to provide the same value with 95% confidence; the final value was averaged over the 10 trials, five from each method.

Wetting Measurements

Wetting measurements were conducted with the FTA200 equipped with the First Ten Angstroms environmental chamber. A VTI RH200 relative humidity generator was used to maintain ~30% relative humidity (using Ultrapure N₂) within the chamber in order to maintain the specimen moisture content at ~6%. The N₂ flowed into the chamber at 500 mL/min and was directed through open-cell foam in order to promote turbulent flow that did not deform the liquid droplet during video recording. A 1 µL resin droplet was placed in the middle of the specimen cross-section surface, and in most cases placement was restricted to earlywood regions except for spotted gum where no practical distinction was possible.

The FTA200 camera was perpendicular to the specimen's longitudinal axis and tilted downwards (3°) to clearly observe the droplet in the middle of the specimen surface; light was reflected into

the chamber to enhance image contrast. Using an adjustable stage, the specimen was raised up to “pluck” or transfer the droplet from the syringe tip to the specimen surface. First Ten Angstroms FTA32 software was used to control video recording (acquisition rate: 1 image/second for pMDI and UF and 1 image/10 seconds for PF PLY and PF OSB; initiated with a grey-scale pixel trigger), and to obtain contact angles averaged from both sides of the droplet. The wetting period was defined as the time from the initial droplet contact on the wood surface until the resin was cured, including specimen transport time. This time was not fixed due to the great variation in wetting behavior observed. To cure the resin, the specimen was either microwaved for 2.5 minutes on 50% power, or immersed in ~15 mL of liquid NH₃ for 10 minutes, where after it was removed and allowed to warm to room temperature. Since it was plausible that microwave heating might promote additional penetration, the liquid NH₃ treatment was devised to terminate pMDI flow more rapidly. Ten replicates were obtained for each wood type.

Statistical Methods

Resin properties and wetting results were compared using a one-way ANOVA comparison and a Tukey’s honestly significant difference (HSD) test for a pairwise comparison between each resin. The statistical analysis was run with a separation of species to determine what the most significant factors were for each species.

2.3 Results and Discussion

Resin Properties

Table 2-1 shows the viscosity, surface tension, and density measurements for the resins studied. All the aqueous resins have surface tensions significantly higher than pMDI. Of the water-borne resins, only PF OSB had viscosity statistically comparable to pMDI; PF PLY and UF had higher viscosities characteristic of their application in plywood. Based upon this table, expectations were that pMDI would behave very differently, whereas the only apparent difference among the water-borne resins was viscosity.

Table 2-1: Liquid properties of the four resins studied; average (stdev)

	Surface Tension (mN/m) (n = 10)	Viscosity (mPa·s) (n = 8-14)	Density (g/mL) (n = 3-4)
pMDI	44.0 (0.3)	228.4 (17.9)	1.23 (0.0)
PF OSB	68.8 (0.8)	245.2 (17.8)	1.22 (0.0)
PF PLY	68.9 (0.6)	864.2 (72.3)	1.19 (0.0)
UF	70.1 (1.3)	879.2 (87.8)	1.26 (0.0)

Wetting Behavior

Figure 2-1 and 2-2 shows typical wetting behavior observed on loblolly pine and Douglas-fir cross-sectional surfaces. Notice that PF OSB exhibited what might be described as idealized, time-dependent wetting behavior on wood; although the initial contact angle exceeded 90°, it gradually declined towards an equilibrium value near 30°. This should be considered favorable wetting, and an indication of a favorable wood/resin interaction. UF and pMDI exhibited an even more favorable wood interaction, where complete penetration and droplet disappearance occurred before an equilibrium contact angle was reached. This rapid resin absorption is common for pMDI (Shi & Gardner, 2001), but it is currently unknown how this behavior impacts bond performance. Figure 2-3 demonstrates typical wetting behavior observed on spotted gum cross-sectional surfaces. The limited examples shown in Figures 2-1 through 2-3 demonstrate that the species exhibited dramatically different surface properties, perhaps most striking in the case of the UF resin. Notice for both woods that the PF PLY specimens appeared to achieve an equilibrium contact angle; but evidence (not shown here) suggested that PF PLY resin droplets formed a skin that impeded contact angle reduction beyond about 150 seconds. Consequently, it was estimated that only the first 150 seconds of the PF PLY data were usable, and that the arbitrary cut-off was not entirely clear based upon observation.

While Figures 2-1 through 2-3 show typical wetting curves, Figure 2-4 is provided to convey the great deal of wetting variation observed with all specimens in this work. It is seen that some droplets formed an equilibrium contact angle, but others did not. This has been attributed to the multiple wood anatomical features and surface energies between the specimens (Kamke & Lee, 2007). Wood anatomy, such as different lumen diameter between earlywood and latewood, can affect wood surface energy; even though this study only observed earlywood wetting, some variability was still expected. The difference in surface energy was based not only on surface

roughness from the lumen diameter, but also on the amount of lignin and polysaccharides present, based on the cell type. This variability is unfortunate because it prevents use of the convenient wetting model (K-parameter) of Shi and Gardner (2001). Instead wetting was evaluated using two parameters: the initial contact angle and the percentage change in contact angle over a period of 35 seconds.

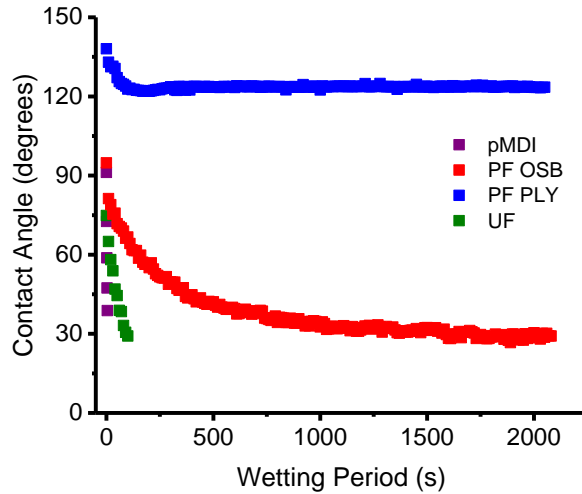


Figure 2-1: Example wetting curves of all resins on loblolly pine cross-sectional surfaces, earlywood. (n = 10-12)

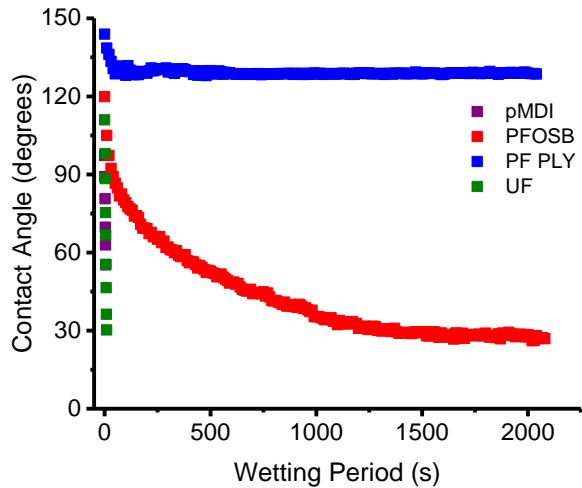


Figure 2-2: Example wetting curves of all resins on Douglas-fir cross-sectional surfaces, earlywood. (n = 10-13)

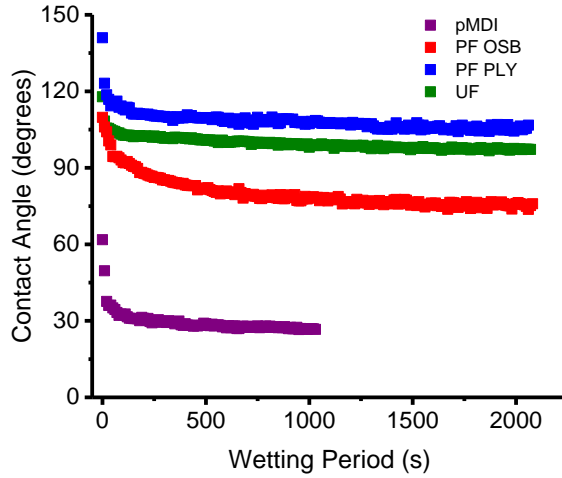


Figure 2-3: Example wetting curves of all resins on spotted gum cross-sectional surfaces, earlywood. (n = 8-14)

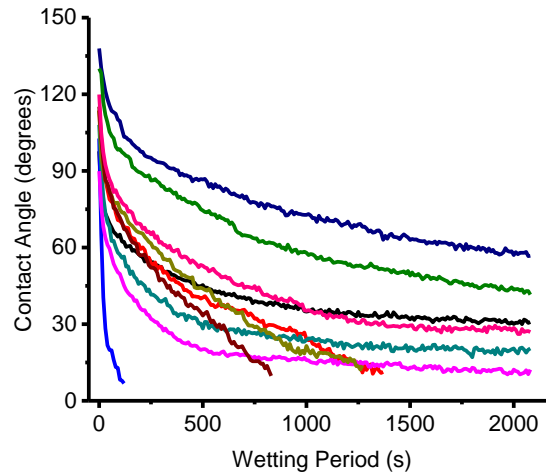


Figure 2-4: Example variation of PF OSB wetting on Douglas-fir cross-sectional surfaces, earlywood (n = 10).

Influence of resin type on wetting behavior

Figure 2-5 summarizes the initial contact angles of all resins observed on the cross-sectional surface of all woods. Within the respective species, and generally, pMDI exhibited the lowest initial contact angle, as expected from its low surface tension. Also, pMDI tended to exhibit favorable wetting (initial contact angle $\leq 90^\circ$). In contrast, the aqueous resins tended to exhibit higher initial contact angles and unfavorable wetting (initial contact angle $\geq 90^\circ$). Since the aqueous resins had practically identical surface tensions (Table 2-1), it was surprising to observe such significant differences in initial contact angles within the respective species. This suggests that specific acid/base interactions might play a role in wetting that is not simply revealed when considering resin surface tension. All three woods exhibited effects from the resins, but UF on loblolly pine cross-section deserves special mention because it was indistinguishable from pMDI. This unique behavior could be explained by Mirabile's findings from a separate study using specimens from the same trees as those used here (2017). He used an acid/base surface model applied to the wetting of pure liquids and found that loblolly pine surface energy was 39% higher than Douglas-fir. Mirabile's findings do not explain the contradictory results found here but taken with the data, it is clear that the UF/loblolly pine wetting phenomena is very complex.

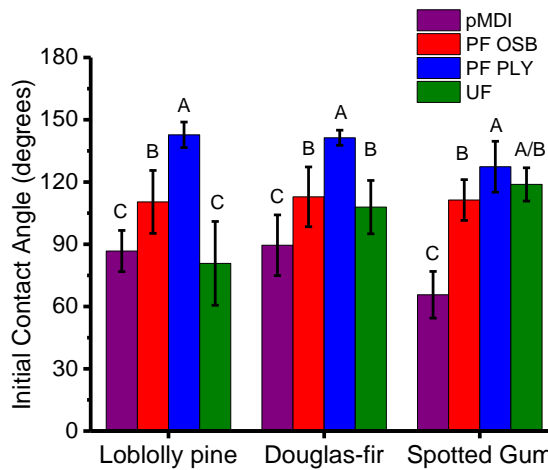


Figure 2-5: Initial contact angle of all resins as a function of species. Statistical significance shown by capital letters, but only within each species. (n = 8-14)

Figure 2-6 summarizes the percent change in contact angles (ΔCA) of all resins observed on the cross-sectional surfaces of all species. pMDI exhibited a significant ΔCA on all species. This change was most likely due to the low surface tension and viscosity, and, as previously mentioned, is a common wetting behavior for pMDI. In comparison, PF OSB and PF PLY did not have significantly different ΔCA ; with the exception of PF OSB on Douglas-fir, where the ΔCA resembled pMDI. Special recognition goes to UF, which was indistinguishable compared to pMDI on both loblolly pine and Douglas-fir. According to Table 2-1, UF had significantly different resin properties from pMDI, therefore the wetting should be significantly different. When comparing UF to PF PLY and PF OSB, UF has an acid catalyst added making the pH much lower than that of the alkaline PF PLY and PF OSB resins. This acidic nature of UF could possibly explain the unexpected wetting behavior observed.

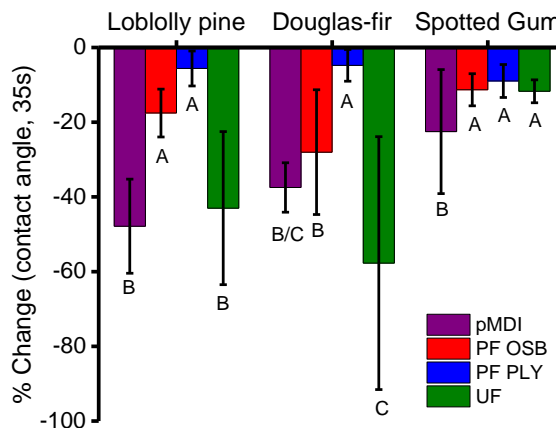


Figure 2-6: Percent change in contact angle of all resins as a function of species. Statistical significance shown by capital letters, but only within each species. (n = 8-14)

Since the initial contact angle of UF on loblolly pine was indistinguishable from pMDI, the significant ΔCA , in Figure 2-6, was expected. However, the ΔCA observed with PF OSB and UF on Douglas-fir (Figure 2-6) was surprising since both resins had unfavorable initial contact angles (Figure 2-5). This suggests that a change occurred as the contact angle advanced on Douglas-fir, as observed with Shi and Gardner (2001). Since both UF and PF OSB were aqueous, the surface tension would decrease as the water transferred into the cell wall, causing a

smaller ΔCA than observed. It is possible that the wood surface energy of Douglas-fir may have changed, causing the favorable ΔCA . Significant ΔCA indicate favorable wetting and lumen penetration (de Meijer, Thurich, et al., 2001; Scheikl & Dunky, 1998; Sernek et al., 2004), therefore stronger wood-adhesive interactions were expected to occur with the systems in Figure 2-6 that exhibited significant ΔCA .

According to the Lucas-Washburn equation (Eq. 2-1), minimal penetration was expected with the aqueous resins because as water transferred into the cell wall, the surface tension and viscosity were expected to change, not favoring penetration, with exception of certain systems with UF and PF OSB. The non-aqueous pMDI resembles a homogeneous liquid, hence it was not expected to interact with the wood, and should penetrate deeper. This could explain the favorable initial contact angle and ΔCA observed with pMDI on all three species.

2.4 Summary

Wetting is a helpful tool to improve the understanding of the wood-adhesive interaction. The wetting behaviors of 4 wood resins were analyzed on 3 wood species. Observations confirmed the hypothesis that the non-aqueous resin would behave differently, as it was the only resin to exhibit favorable wetting on all three species. It was demonstrated that the aqueous resins had unfavorable wetting with the exception of UF and PF OSB on Douglas-fir and UF on loblolly pine. The favorable wetting of UF was unexpected and could be attributed to the acidic nature of the resin. Findings suggest that changes occurred within Douglas-fir as the wetting progressed from unfavorable to favorable. Since the UF wetting was different than expected, further research is suggested with UF wetting and penetration. The implications on wood-adhesive interactions were that pMDI would penetrate rapidly; whereas the aqueous adhesives would have minimal penetration, with the exception of PF OSB and UF on Douglas-fir and UF on loblolly pine. The general behavior of this research agreed with Shi and Gardner (2001).

References

Barbu, M. J., Reh, R., & Irle, M. (2014). Wood-Based Composites. In A. D. Aguilera, J. Paulo (Ed.), *Research Developments in Wood Engineering and Technology* (pp. 1-45). Hershey, PA: Engineering Science Reference (an imprint of IGI Global).

Berg, J. C. (2010). *An Introduction to Interfaces and Colloids: The Bridge to Nanoscience*. Tuck Link, Singapore: World Scientific Publishing Co. Pte. Ltd.

de Meijer, M., Thurich, K., & Militz, H. (2001). Quantitative measurements of capillary coating penetration in relation to wood and coating properties. *Holz als Roh- und Werkstoff*, 59, 35-45.

Gavrilović-Grmuša, I., Dunky, M., Miljković, J., & Djiporović-Momčilović, M. (2010). Radial Penetration of Urea-Formaldehyde Adhesive Resins into Beech (*Fagus Moesiaca*). *Journal of Adhesion Science and Technology*, 24(8-10), 1753-1768. doi:10.1163/016942410x507812

Johnson, S. E., & Kamke, F. A. (1992). Quantitative Analysis of Gross Adhesive Penetration in Wood Using Fluorescence Microscopy. *The Journal of Adhesion*, 40(1), 47-61. doi:10.1080/00218469208030470

Kamke, F. A., & Lee, J. N. (2007). Adhesive Penetration in wood- A Review. *Wood and Fiber Science*, 39(2), 205-220.

Lucas, R. (1918). Ueber das Zeitgesetz des kapillaren Aufstiegs von Flüssigkeiten. *Kolloid-Zeitschrift*, 23, 15-22.

Maloney, T. M. (1996). The family of wood composite materials. *Forest Products Journal*, 46(2), 19-26.

Mirable, K. V., & Zink-Sharp, A. (2017). Fundamental bonding properties of Douglas-fir and southern yellow pine wood. *Forest Products Journal*, In-Press. doi:<https://doi.org/10.13073/FPJ-D-17-00019>

Scheikl, M., & Dunky, M. (1998). Measurement of Dynamic and Static Contact Angles on Wood for the determination of its Surface Tension and the Penetration of Liquids into the wood Surface. *Holzforschung*, 52(1), 89-94.

Sernek, M., Kamke, F. A., & Glasser, W. G. (2004). Comparative analysis of inactivated wood surface.

Shi, S. Q., & Gardner, D., J. (2001). Dynamic adhesive wettability of wood. *Wood and Fiber Science*, 33(1), 58-68.

Washburn, E. W. (1921). The Dynamics of Capillary Flow. *Physical Review*, 17(3), 273-283.
doi:10.1103/PhysRev.17.273

Yang, X., & Frazier, C. (2016). Influence of organic fillers of surface tension of phenol-formaldehyde adhesives. *International Journal of Adhesion and Adhesives*, 66, 160-166.

3. Applicability of the Lucas-Washburn Equation for predicting pMDI penetration

Abstract:

The penetration of non-aqueous resins into wood has been investigated previously, but has not been compared to the wetting behavior. Therefore, to give a more thorough analysis, this research compared the wetting and penetration of polymeric (methylene diphenyl diisocyanate) (pMDI) on 5 wood species. Wetting was analyzed with the sessile drop method, which observed the initial contact angle and change in contact angle over 35s; penetration was measured within each individual tracheid. It was proposed that the change in contact angle gave more valuable information than the initial contact angle. The wetting behaviors exhibited grain and species effects, which had implications on the resin availability for flake/strand-based composite products. The Lucas-Washburn equation was used to analyze the wetting and penetration, by calculating the penetration and comparing it to the measured penetration. The greater surface energy of loblolly pine most likely accounted for the significantly greater penetration of loblolly pine compared to Douglas-fir. The Lucas-Washburn calculated penetration exceeded the measured penetration, but since penetration was predicted the hypothesis was still considered successful.

Keywords: Wetting, wood-based composites, penetration, pMDI, Lucas-Washburn equation

3.1 Introduction

Society's value of wood-based composites continues to grow under typical competitive and regulatory pressures. While the industry has been operating for over a century (Barbu et al., 2014; Maloney, 1996), the wood-adhesive interaction remains poorly understood. It is well-known that bond performance is directly related to adhesive wetting and subsequent penetration, but it has been difficult to find quantitative relationships between wetting, penetration and performance (Kamke & Lee, 2007).

Wetting is affected by liquid surface tension and solid surface energy (Berg, 2010), and is commonly defined as either favorable or unfavorable if the contact angle is respectively less than or greater than 90°. Correspondingly, for porous substrates such as wood, the Young-Laplace

relationship predicts that capillary uptake occurs when wetting is favorable; but not so when wetting is unfavorable (Berg, 2010). The Young-Laplace relationship does not account for liquid viscosity, but this is accounted for in the Lucas-Washburn equation (Lucas, 1918; Washburn, 1921), Equation 3-1, where the penetration distance, h , is related to the capillary radius, r , liquid surface tension, γ , liquid viscosity, η , the contact angle θ , and time, t .

$$h^2 = \frac{r\gamma \cos \theta}{2\eta} t \quad (3-1)$$

There have been many studies that correlate wetting behavior to adhesive or coating penetration (Scheickl & Dunky, 1998; Shi & Gardner, 2001; Szekely et al., 1970), but few compare the actual penetration to the predicted penetration (de Meijer, Thurich, et al., 2001). The focus of this research was to improve the understanding of adhesive wetting of, and the subsequent penetration into, wood. This work only considers penetration due to capillary forces, the events prior to bond consolidation and compaction.

3.2 Materials and Methods

Materials

Polymeric (methylene diphenyl diisocyanate) (pMDI) Rubinate M ®, was obtained from Huntsman Polyurethanes. Five different wood species were obtained in the form of air-dried lumber: loblolly pine (*Pinus taeda*) from Critz, Virginia, USA; Douglas-fir (*Pseudotsuga menziesii*) from Benton, Oregon, USA; yellow-poplar (*Liriodendron tulipifera*) from Virginia, USA; European beech (*Fagus sylvatica*) from Germany; and spotted gum (*Corymbia citriodora*) from Queensland, Australia. Specimens were rough-cut into ~9 mm³ cubes (attempting to obtain zero grain angle on the side grain surfaces), saturated in distilled water, and then microtomed (GSL1 sliding microtome) on all surfaces. The specimens were dried by cycling between vacuum (0.15 mmHg) and dry N₂ three times, and stored with dry N₂/molecular sieves. Specimens were then equilibrated to ~6% moisture content in a desiccator over a saturated magnesium chloride solution.

Resin viscosity

A TA Instruments AR G2 Rheometer was used (concentric cylinder, diameter = 30.35 mm, gap = 1 mm) to obtain steady-state flow curves (25°C; 0.5 to 3000 s⁻¹; ramping up in shear, then ramping down with no delay between ramps; steady-state criteria = 3 consecutive data points collected in 1 minute or less, shear stress ≤ 5% change).

Resin surface tension

Resin density was measured using a 10 mL graduated cylinder. Approximately one milliliter increments were added using a syringe and the density was obtained from the linear slope of the mass/volume plot; the corresponding correlation coefficients (R²) were always above 0.99.

Surface tension was measured by the drop shape and drop weight methods at room temperature with a First Ten Angstroms, FTA 200, as described by Yang and Frazier (2016). The surface tension reported below was from 10 observations analyzed separately using the drop shape and drop weight methods. The separate results of the drop shape and drop weight methods were not significantly different; the final surface tension was averaged over 10 results, five from each method.

Wetting Measurements

Wetting measurements were conducted with the FTA200 equipped with the First Ten Angstroms environmental chamber. A VTI RH200 relative humidity generator was used to maintain ~30% relative humidity (using Ultrapure N₂) within the chamber in order to maintain the specimen moisture content at ~6%. The N₂ flowed into the chamber (500 mL/min) and was directed through open-cell foam in order to promote turbulent flow that did not deform the liquid droplet during video recording. A 1 μL resin droplet was placed in the middle of the specimen surface. On the cross-section (end grain) surfaces, droplet placement was restricted to earlywood regions, with exception of an earlywood and latewood comparison on Douglas-fir, and of spotted gum, where no practical distinction was possible. On side grain surfaces, no distinction between earlywood and latewood was made, and this effect was considered random.

The FTA200 camera was perpendicular to the specimen's longitudinal axis and tilted downwards (3°) to clearly observe the droplet in the middle of the specimen surface; light was reflected into

the chamber to enhance image contrast. Using an adjustable stage, the specimen was raised up to “pluck” or transfer the droplet from the syringe tip to the specimen surface. First Ten Angstroms FTA32 software was used to control video recording (acquisition rate: 1 image/10 seconds for side grain and 1 image/second for end grain; initiated with a grey-scale pixel trigger), and to obtain contact angles averaged from both sides of the droplet. The video recording time (wetting period) was not fixed and was defined as the time from droplet deposition, through wetting, and until the droplet was cured; this wetting period included an adjustment for specimen handling. At the end of the wetting period, the resin was cured by immersing the specimen into ~15 mL of liquid NH₃ for a period of 10 minutes, whereafter it was removed and allowed to warm to room temperature. The liquid NH₃ treatment was devised to terminate pMDI flow more rapidly, in order to minimize resin penetration. Ten replicates were obtained for each wood type.

Penetration Measurements

After the resin was cured with NH₃, specimens were vacuum/pressure soaked in water and microtomed (GSL1 sliding microtome) to obtain 6-7 sections, 20-25 μm thick, nearest to the droplet center. The sections were rinsed with DI water and stained with a 0.5% safranin solution. Penetration was observed using a Nikon DS Fi-1 camera (Nikon Eclipse LV microscope) with a G-2A filter cube (excitation range of 510-560 nm; fluorescence emission range ≥ 590 nm), and length measurements were made using NIS BR Elements Software. A preliminary screening identified the section having the deepest resin penetration. Within that single section, the penetration within isolated tracheid cells (specific penetration) was measured, and the average lumen diameter was obtained from 3 locations within each tracheid measured (13-71 cells per section).

Statistical Methods

Resin properties and wetting results were compared using a one-way ANOVA comparison and a Tukey’s honestly significant difference (HSD) test for a pairwise comparison between each resin. The statistical analysis was run with a separation of species to determine what the most significant factors were for each species.

3.3 Results and Discussion

Wetting

The average viscosity and surface tension of the pMDI used in this work were 228.4 mPa·s (± 17.9) and 44.0 mN/m (± 0.3) respectively. Figures 3-1 to 3-3 demonstrate typical wetting curves for different grain and tree species. While these are typical curves, note that a great deal of variation was observed within each species/grain combination, as shown in Figure 3-4 for example. On most species, pMDI wetting was favorable (initial contact angle $\leq 90^\circ$). After initial contact, pMDI droplets tended towards three general behaviors: 1) single-stage (i.e. one discernable slope in the wetting curve) rapid reduction due to capillary wicking or 2) two-stage, a rapid reduction followed by little or no change as if an equilibrium is approached, or 3) single-stage, gradual reduction. Besides a contact angle $< 90^\circ$, favorable wood/resin interactions promote rapid reductions in contact angle. Single-stage rapid reduction due to capillary wicking represents the “strongest” wood/resin interaction, but this type of wetting may or may not prove beneficial to product performance. In fact, it is currently unknown how pMDI wetting behavior impacts industrial production. In the resin blender, one envisions that wetting behaviors 2 or 3 would promote resin redistribution through mechanical action in the blending process. On the other hand, single-stage rapid capillary wicking of resin might have a greater impact on bulk wood properties (filling lumens and slightly swelling the cell wall) as opposed to interfacial bonding effects.

Apparent in Figures 3-1 to 3-4 is that the experimental wetting period was not fixed because wetting was so highly variable among the species studied. Since the time variable appeared in the Lucas-Washburn equation (hereafter referred to as Washburn), it was unnecessary to fix the wetting period; but it must be correctly measured to compare Washburn predictions with experimental measurements. Figures 3-1 to 3-4 also demonstrate that in many cases the pMDI droplet was completely absorbed into the substrate before exhibiting an equilibrium contact angle. This was unfortunate because the beneficial wetting model (K-parameter) of Shi and Gardner (2001) could not be used in this work. Instead, wetting was evaluated using two parameters: the initial contact angle and the percentage change in contact angle over a period of 35 seconds.

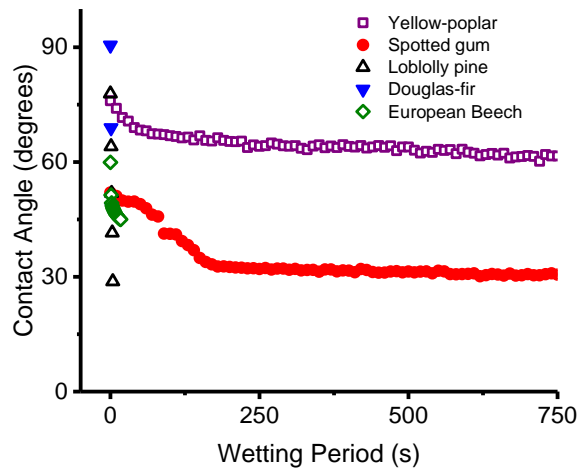


Figure 3-1: Example wetting curves of pMDI on the cross-sectional surface of all five species. (n = 10-14)

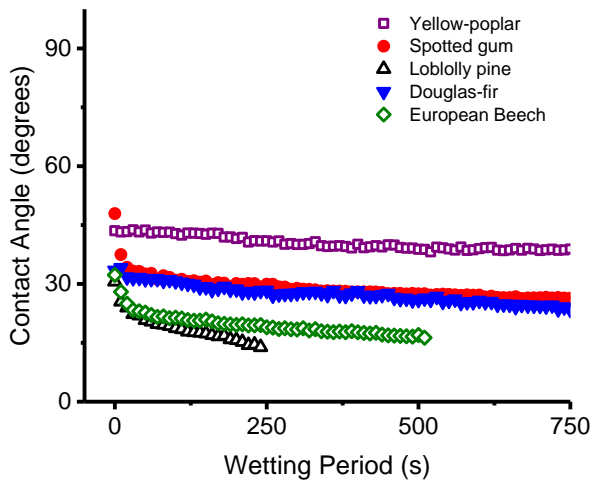


Figure 3-2: Example wetting curves of pMDI on the tangential surface of all five species. (n = 10)

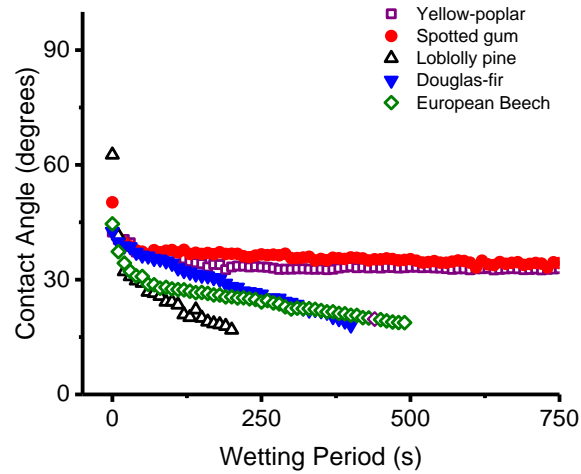


Figure 3-3: Example wetting curves of pMDI on the radial surface of all five species. (n = 10)

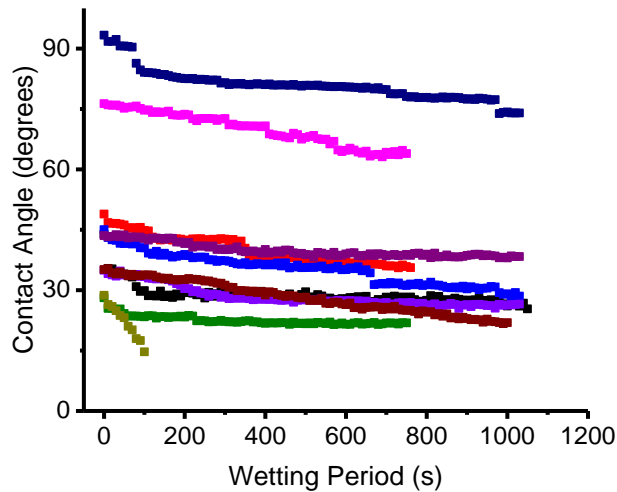


Figure 3-4: Example variation of pMDI wetting on the tangential surface of yellow-poplar (n = 10).

Grain orientation and pMDI wetting

Figure 3-5 shows that cross-sectional (end grain) surfaces exhibited significantly higher initial contact angles than side grain surfaces (radial and tangential), consistent with de Meijer et al. (2000) and Shi and Gardner (2001). Among the woods studied, only spotted gum exhibited three, significantly distinct surface effects. Otherwise the radial and tangential surfaces had

indistinguishable wetting among all other woods. A direct comparison to de Meijer et al. (2000) and Shi and Gardner (2001) was not possible because both simply quantified an end grain versus side grain effect. However, Gavrilovic-Grmusa et al. compared radial and tangential wetting with urea-formaldehyde resin (species studied: beech (*Fagus moesiaca*), fir (*Abies alba*) and poplar (*Populus euramericana*)) and did not find a significant difference between the two surfaces (2013), consistent with the results of this study.

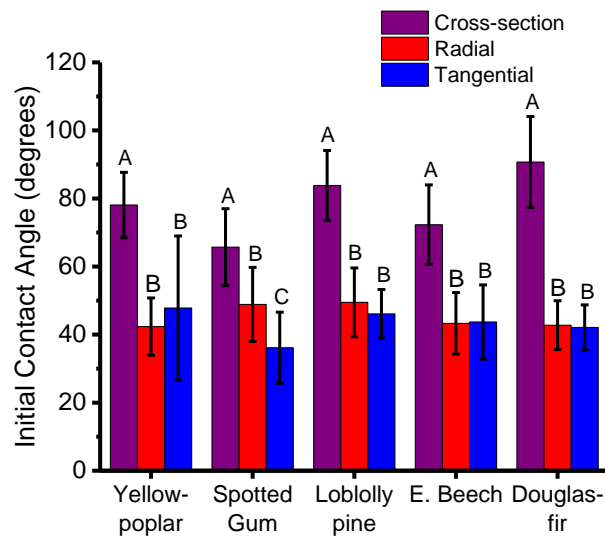


Figure 3-5: pMDI initial contact angles as a function of grain and species. Statistical significance shown by capital letters, but only within each species. (n = 10-14)

Regarding percent change in contact angle (ΔCA), spotted gum and yellow-poplar stood out as exhibiting no grain effects, and relatively low ΔCA , Figure 3-6. Spotted gum is known for the presence of tyloses (Burch, 2015), which limit or preclude penetration. However yellow-poplar has open vessels and so it is not clear why this wood exhibited the lowest ΔCA . Note that Gavrilovic-Grmusa et al., (2013) found that yellow-poplar exhibited greater ΔCA values (pMDI) than Balkan Beech (*Fagus moesiaca*), contradicting the similar yellow-poplar/European Beech (*Fagus sylvatica*) comparison here and again, this seems to make the yellow-poplar/spotted gum comparison even more confounding.

Likewise, loblolly pine, European Beech and Douglas-fir all exhibited grain effects, and relatively greater ΔCA , indicating (or suggestive of) lumen penetration (Berg, 2010). Even with careful attention to specimen preparation there will be open, accessible lumens, effectively end grain features on side grain surfaces. These features allow for capillary uptake and therefore may cause a reduction in contact angle when wetting is favorable. In the absence of end grain features (open lumens) the resin cannot penetrate in the time scale of the observation.

Recall that side grain surfaces were prepared with no control over earlywood/latewood location. As in this case, randomizing that effect was expected to increase the variability of ΔCA values on side grain surfaces. Of the woods studied here, the comparison of loblolly pine and Douglas-fir is most interesting because the two woods exhibit significantly different ΔCA . The representative tracheid diameters were identical ($p = 0.555$), so the difference in ΔCA was unrelated to the diameter of end grain features appearing on side grain surfaces. Since the initial contact angles on the side grains of loblolly pine and Douglas-fir were effectively the same, Figure 3-5, it seemed that more information was attained from ΔCA than the initial contact angle; however the exact benefit of the ΔCA remains in question. Burch's thesis also found that time dependent wetting was more informative, but that initial contact angles were still useful (2015). Note that Scheikl and Dunky found that earlywood had better wetting properties (urea-formaldehyde resins on tangential surfaces) due to larger lumen diameter causing a greater surface roughness (1998). However they provided no information about data variation, so it is difficult to assess this claim.

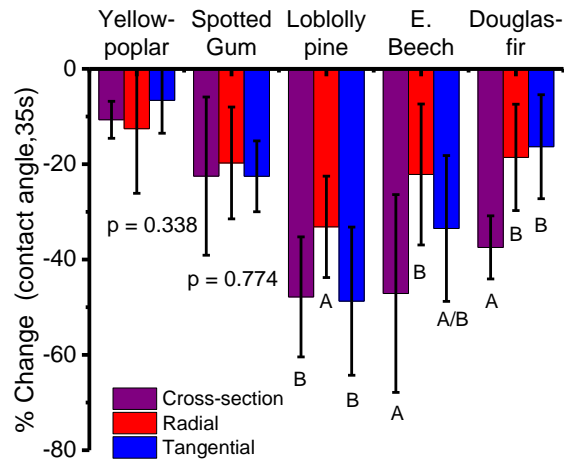


Figure 3-6: Percent change in pMDI contact angles as a function of species and grain. Statistical significance shown by capital letters, but only within each species. (n = 10-14)

Earlywood and latewood effects were compared on cross-sectional surfaces, Table 3-1. Earlywood exhibited significantly greater initial contact angles (indicative of less favorable wetting) and greater ΔCA (indicative of more favorable wood/resin interaction). The conflicting implications seem to again suggest greater insight was gained from ΔCA than from the initial contact angle. However given the complexity of wood/resin interactions demonstrated here and by others (Gavrilovic-Grmusa et al., 2013; Shi & Gardner, 2001), it would be unwise to omit reports of the initial contact angle. Finally, given that earlywood exhibited more favorable wood/resin interactions (greater ΔCA), it is reasonable to expect that earlywood/latewood effects on side grain surfaces would also occur, as with Scheickl and Dunky’s findings (urea-formaldehyde resins on tangential surfaces) (1998).

Table 3-1: Pair-wise comparison of Douglas-fir earlywood and latewood wetting. (n = 10)

	Initial Contact Angle (degrees)	% Change in Contact Angle
Earlywood	89.5 (14.6)	-72.48 (5.7)
Latewood	74.5 (7.4)	-49.1 (7.7)
Pair-wise comparison	p = 0.005	p = 0.000

Species effects and pMDI wetting

Referring to Figure 3-7, the initial contact angles exhibited a species effect, but only on end grain surfaces; there was no distinguishable difference between the side grains of all species. Note that while the relationship between wetting and penetration is the principal focus, this work has implications for the industrial practice of resin/flake blending. While the wetting periods here are much longer than the timescale for particle collisions in the resin blender, the wetting behaviors exhibited here must certainly influence resin blender efficiency and resin distribution. The initial contact angle and ΔCA , relates to the size of droplets and their residence time on the flake surface during resin blending. For instance, larger droplets with longer residence time have greater availability for mechanical transfer to other flakes in the blending process. For flake or strand-based products, the intention is to machine flakes from the tangential surface, but there are deviations such that a mixture of tangential and radial surfaces is created. In this regard, Figure 3-7 suggests that initial contact angle would not be affected by flake/strand imperfections involving the variation between tangential and radial grain patterns.

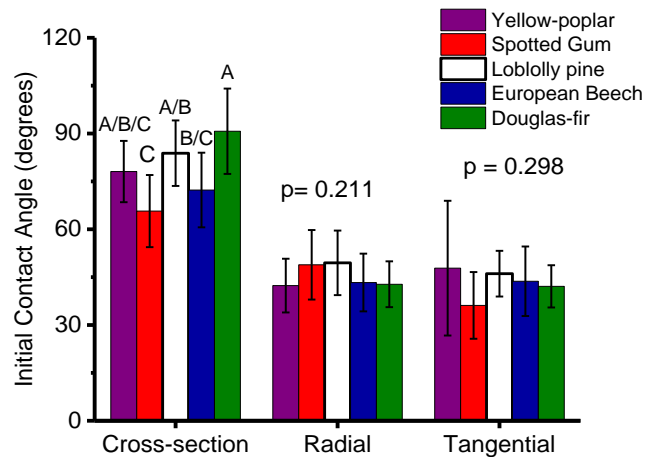


Figure 3-7: Initial contact angle of pMDI as a function of species and grain orientation.

Statistical significance shown by capital letters, but only within each surface type. (n = 10-14)

However for ΔCA , Figure 3-8, a species effect was observed on all three surfaces, in agreement with Shi and Gardner (2001). In relation to resin/flake blending, Figure 3-8 suggests that, the

Δ CA would be affected by flake/strand imperfections. Consequently, these results suggest that resin blender efficiency and the related resin distribution on flakes/strands could vary as a function of tree species and grain imperfections (i.e. deviation from a purely tangential flake surface).

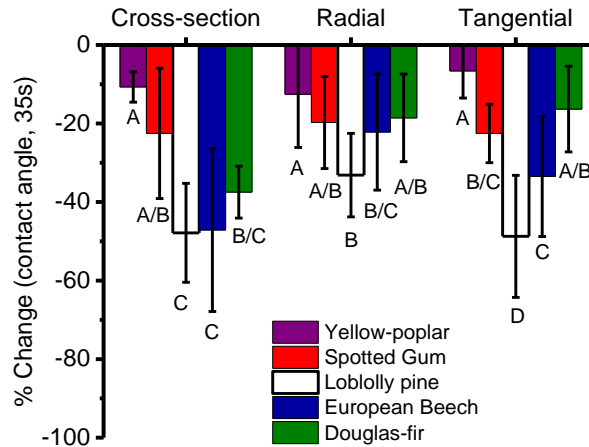


Figure 3-8: Percent change in pMDI contact angles as a function of species and grain orientation. Statistical significance shown by capital letters, but only within each surface type. (n = 10-14)

It is well known that wetting can impact penetration (Liptáková & Kudela, 1994; Scheickl & Dunky, 1998; Shi & Gardner, 2001). De Meijer (2001) defined three general wetting behaviors: 1) stable droplet diameter and height with minimal contact angle and volume change 2) stable droplet diameter with a height, contact angle, and volume decrease; attributed to lumen penetration 3) droplet diameter, height and contact angle decrease; attributed to both favorable wetting and lumen penetration. Using these definitions the most commonly observed wetting behavior in this work was case 3 (data not shown), indicating that favorable wetting and capillary penetration occurred.

Penetration prediction via the Washburn equation

Specific penetration was defined as penetration depth measured within individual tracheids and was accompanied by lumen diameter measurements in three locations along the cell length, so as

to enable penetration predictions. According to the Washburn equation, if pMDI wetting on these woods is the same, the corresponding resin penetration should be identical since the lumen diameters were the same ($p = 0.555$). Figure 3-9 shows that the pMDI wetting behavior on loblolly pine and Douglas-fir was not significantly different, therefore pMDI penetration into these woods should be similar.

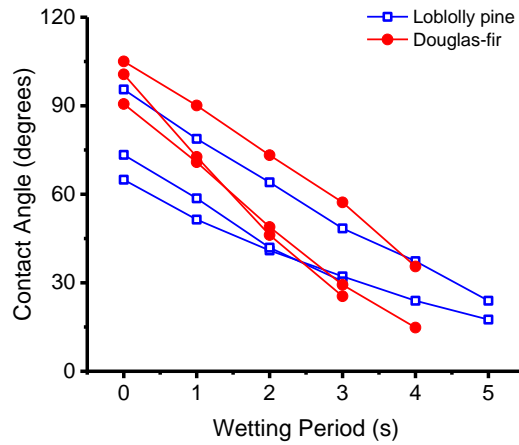


Figure 3-9: Example wetting curves of pMDI on Douglas-fir and loblolly pine. ($n = 10$)

The rapid decrease in contact angle observed in Figure 3-9, indicates favorable wetting for both species. However, it is important to note that the total wetting period was 12-15 seconds, to account for the specimen transport time. As a parameter of the Washburn equation, time was not controlled, but it must be correctly measured to compare Washburn predictions with experimental measurements. Based on this negative slope, the contact angle should be 0° by the time cure was initiated, indicating complete wetting; therefore in the Lucas-Washburn calculations, $\cos(0^\circ) = 1$.

When comparing only the measured penetration in Figure 3-10, loblolly pine was significantly greater than Douglas-fir ($p = 0.003$; $DF = 692$). This finding is in contradiction to those of Shi and Gardner (2001), however they did not measure penetration; they surmised a qualitative understanding of penetration through K-value measurements on tangential surfaces.

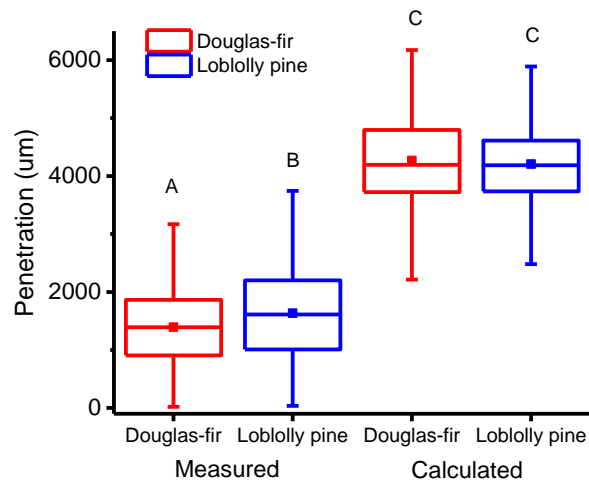


Figure 3-10: Boxplots comparing the calculated and measured penetration of pMDI resin into loblolly pine and Douglas-fir cross-sectional surfaces. Statistical significance shown by capital letters. (Whiskers: 5th & 95th percentile; open box: 25th & 75th percentile; line: median; closed square: mean) (n = 18-48 cells per slide with n = 10 slides per species)

It seems unlikely that the minor difference in pMDI wetting on these woods (Δ CA on tangential surfaces, Figure 3-5) could explain the difference in measured penetration. On the other hand, the loblolly pine surface energy could be substantially higher than Douglas-fir. That was Mirabile's finding in his thesis work which used specimens from the same trees as those used here (2017). Using an acid/base surface model applied to the wetting of pure liquids, Mirabile found that loblolly pine surface energy was 39% higher than Douglas-fir. Mirabile's findings do not explain the contradictory results found here, but taken with the data herein it is clear that resin/wood wetting and penetration phenomena are very complex.

Another factor that could attribute to this difference was the average tracheid length between the species. Previous studies show the average tracheid length for mature Douglas-fir was 3.1-3.5 mm (Bannan, 1965; Fabisiak & Molinski, 2002), and the average tracheid length for mature loblolly pine was 3.9-4.2 mm (Larson et al., 2001; Taylor & Moore, 1981). Due to the significantly different average tracheid lengths between the species ($p = 0.021$), Douglas-fir should have less penetration than loblolly pine, which was consistent with the measured penetration results (Figure 3-10). However, in comparison to the normal distribution of the

calculated penetration, Figure 3-10, the boxes representing the measured penetration are skewed lower. If the tracheid length was in fact the limiting factor, the box should be skewed higher. Considering all observations here, it is safe to conclude that the pMDI/wood interactions are significantly different on the respective woods, and that the tracheid length was not the limiting factor. It would be interesting to compare these woods according to their swelling behavior in pMDI; as wood swells to a minor degree in pMDI (Frazier, 2003).

Figure 3-10 also demonstrated that the calculated penetration exceeded the measured penetration by about a factor of two, which was unexpected. Considering that pMDI resembles a pure liquid, it should have minimal interaction with wood and closely follow the penetration calculated by the Washburn equation. However, the Washburn equation did not account for the average tracheid length. Douglas-fir had significantly greater average calculated penetration compared to the average tracheid length ($p = 0.077$), and the calculated penetration for loblolly pine was indistinguishable from the average tracheid length. Since there was no limit to the penetration calculated in the Washburn equation, the calculations could be greater than physically possible, which would also help explain why the calculations exceeded measured penetration.

Figure 3-10 showed that the calculated penetration did in fact predict seemingly identical penetration between the species, which was expected based on the similar lumen diameters ($p = 0.555$). A positive correlation was observed between lumen diameter and measured penetration for loblolly pine (similar to Douglas-fir, not shown), in Figure 3-11. This positive trend validates the Washburn equation assumption (Eq. 3-1) that penetration should be greater with a larger lumen diameter.

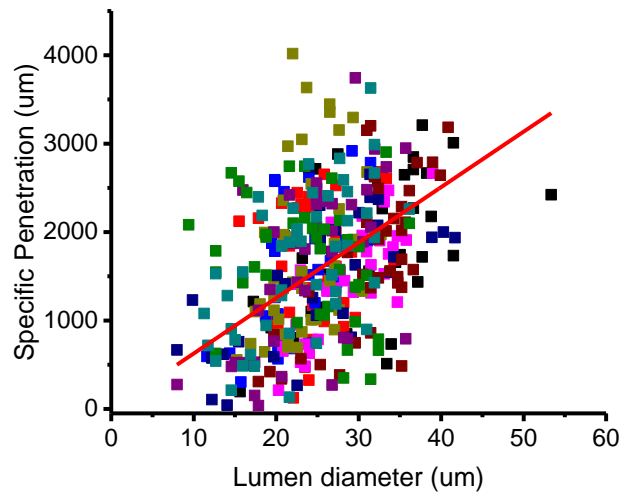


Figure 3-11: Correlation of specific penetration vs lumen diameter on loblolly pine earlywood ($R^2 = 0.85$); each color represents one section ($n = 10$)

Another factor to take into consideration was the assumption of 0° contact angle. Referring back to Figure 3-9, the contact angle chosen was based off the decreasing slope that indicated the contact angle would be at or close to 0° when curing was initiated. However, this assumption may have played a role in the difference between the calculated penetration and the measured penetration. Therefore, using the Washburn equation (Eq. 3-1) the contact angle was solved for, and a scatter plot for loblolly pine is shown in Figure 3-12 (similar for Douglas-fir, not shown). The predicted contact angles approach but never equal 90° , which agrees with the Washburn equation, that any contact angle $\geq 90^\circ$ would indicate no penetration.

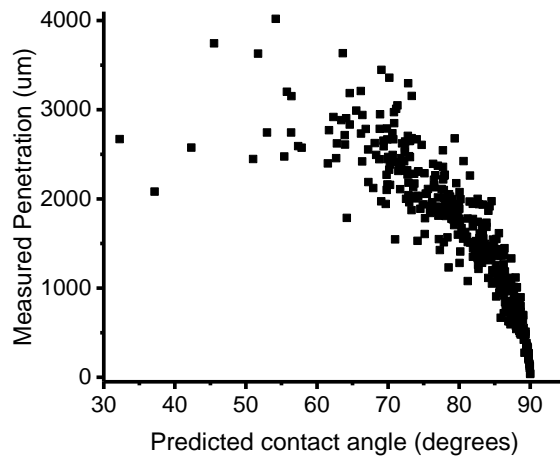


Figure 3-12: Calculated contact angle vs measured penetration on loblolly pine. (n=10)

From Figure 3-12 and Figure 3-13, we can see that the average contact angle that would equate to the measured penetration was 79° for loblolly pine and 82° for Douglas-fir, vastly different from the 0° angle that was assumed for the calculations. This suggests the discussion of what contact angle should be used in the Washburn equation, since an equilibrium contact angle was not reached. This difference also might indicate that wood/resin interactions occurred during penetration, causing the lower penetration than would be expected from the observed wetting. From Figure 3-9, it is unknown exactly how the contact angle of $\sim 80^\circ$ would be chosen, since the wetting rapidly decreased.

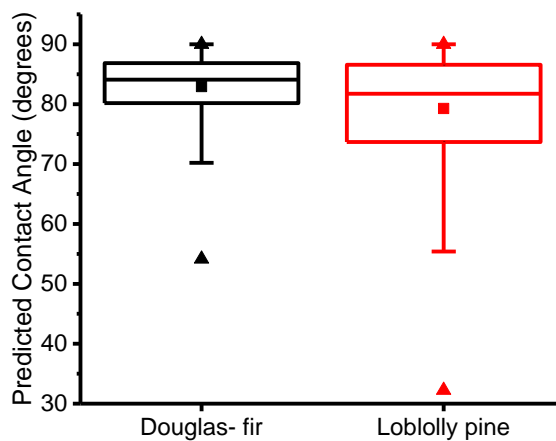


Figure 3-13: Box plot comparing the predicted contact angles of Douglas-fir and loblolly pine. (Closed triangles: min and max; whiskers: 5th & 95th percentile; open box: 25th & 75th percentile; line: median; closed square: mean) (n =18-48 cells per slide with n = 10 slides per species)

The remaining parameters of the Washburn equation, liquid surface tension and viscosity, could have changed during the wetting process, influencing penetration. As soon as pMDI contacts the specimen, the surface tension would change due to the extractives present on the surface of the wood. If during penetration, the monomer infiltrated the cell wall (Frazier, 2003; Zheng et al., 2004), more oligomers would be present in the lumens, increasing the surface tension and viscosity. However, in the 12-15 seconds, cell wall penetration would likely not occur, therefore it was only likely that the surface tension changed from contact.

3.4 Summary

Although it is known that wetting can impact penetration, little research has been done to compare wetting and penetration. The wetting of pMDI on 5 wood species and the penetration of pMDI into two of those species were analyzed. It was suggested that more information was obtained from the ΔCA compared to the initial contact angle. Most woods exhibited favorable wetting; species effects and grain effects were observed, consistent with prior results. The species effects had implications on resin/flake blending efficiency and distribution. Findings suggest that the significantly greater penetration observed with loblolly pine was attributed to the greater surface energy of loblolly pine. Even though the measured pMDI penetration was less than the calculated penetration, the hypothesis was still supported since the prediction was only off by a factor of two. This was likely a result of the fact that the Washburn equation did not account for the average tracheid length, the assumed contact angle of 0° was incorrect, and that the measured penetration was not limited by the tracheid length. Considering pMDI is the resin that best resembles a homogeneous liquid and penetration was not as expected, these findings validated the earlier statement that the wood adhesive interaction is not fully understood. Further research is suggested to better understand the Washburn equation in relation to the pMDI/wood system.

References

- Bannan, M. W. (1965). The length, tangential diameter, and length/width ratio of conifer tracheids. *Canadian Journal of Botany*, 43, 967-984.
- Barbu, M. J., Reh, R., & Irle, M. (2014). Wood-based composites. In A. D. Aguilera, J. Paulo (Ed.), *Research Developments in Wood Engineering and Technology* (pp. 1-45). Hershey, PA: Engineering Science Reference (an imprint of IGI Global).
- Berg, J. C. (2010). *An Introduction to Interfaces and Colloids: The Bridge to Nanoscience*. Tuck Link, Singapore: World Scientific Publishing Co. Pte. Ltd.
- Burch, C. (2015). *Adhesion fundamentals of spotted gum (Corymbia citriodora)*. (Masters of Science Master's of Science), Virginia Tech, Blacksburg, VA.
- de Meijer, M., Haemers, S., Cobben, W., & Militz, H. (2000). Surface energy determinations of woods: Comparison of methods and wood species. *Langmuir*, 16, 9352-9359.
- de Meijer, M., Thurich, K., & Militz, H. (2001). Quantitative measurements of capillary coating penetration in relation to wood and coating properties. *Holz als Roh- und Werkstoff*, 59, 35-45.
- Fabisiak, E., & Molinski, W. (2002). The density and length of tracheids of Douglas-fir (*Pseudotsuga menziesii* Franco) in relation to the biosocial position of a given tree in the stand. *Folia Forestalia Polonica*, B(33), 25-31.
- Frazier, C. E. (2003). Isocyanate Wood Binders. In A. M. Pizzi, K. L. (Ed.), *Handbook of Adhesive Technology, Revised and Expanded* (Vol. 2, pp. 681-694). New York, NY: Marcel Dekker Inc.
- Gardner, D. J., Generalla, N. C., Gunnells, D. W., & Wolcott, M. P. (1991). Dynamic wettability of wood. *Langmuir*, 7, 2498-2502.
- Gavrilovic-Grmusca, I., Djiporovic-Momcilovic, M., Popovic, M., Popovic, J., & Medved, S. (2013). Wetting properties of beech, fir, and poplar interactions with different molar-mass urea formaldehyde resins. *Pro Ligno*, 9(4), 133-143.

- Johnson, S. E., & Kamke, F. A. (1992). Quantitative analysis of gross adhesive penetration in wood using fluorescence microscopy. *The Journal of Adhesion*, 40(1), 47-61.
doi:10.1080/00218469208030470
- Kamke, F. A., & Lee, J. N. (2007). Adhesive penetration in wood- A review. *Wood and Fiber Science*, 39(2), 205-220.
- Larson, P. R., Kretschmann, D. E., Clark III, A., & Isebrands, J. G. (2001). *Formation and properties of juvenile wood in southern pines: A synopsis*. Retrieved from Gen. Tech. Rep. FPL-GTR-129. U.S. Department of Agriculture, Forest Service, Forest Products Laboratory:
- Liptáková, E., & Kudela, J. (1994). Analysis of the wood-wetting process. *Holzforschung*, 48, 139-144.
- Lucas, R. (1918). Ueber das zeitgesetz des kapillaren aufstiegs von flüssigkeiten. *Kolloid-Zeitschrift*, 23, 15-22.
- Maloney, T. M. (1996). The family of wood composite materials. *Forest Products Journal*, 46(2), 19-26.
- Mirable, K. V., & Zink-Sharp, A. (2017). Fundamental bonding properties of Douglas-fir and southern yellow pine wood. *Forest Products Journal*, In-Press. doi:<https://doi.org/10.13073/FPJ-D-17-00019>
- Paris, J. L., & Kamke, F. A. (2015). Quantitative wood-adhesive penetration with X-ray computed tomography. *International Journal of Adhesion and Adhesives*, 61, 71-80.
- Scheikl, M., & Dunky, M. (1998). Measurement of dynamic and static contact angles on wood for the determination of its surface tension and the penetration of liquids into the wood surface. *Holzforschung*, 52(1), 89-94.
- Sernek, M., Kamke, F. A., & Glasser, W. G. (2004). Comparative analysis of inactivated wood surface.
- Shi, S. Q., & Gardner, D., J. (2001). Dynamic adhesive wettability of wood. *Wood and Fiber Science*, 33(1), 58-68.

Szekely, J., Neumann, A. W., & Chuang, Y. K. (1970). Rate of capillary penetration and the applicability of the washburn equation. *Journal of Colloid and Interfacial Science*, 35(2), 273-278.

Taylor, F. W., & Moore, J. S. (1981). A comparison of earlywood and latewood tracheid lengths of loblolly pine. *Wood and Fiber Science*, 13(3), 159-165.

Washburn, E. W. (1921). The dynamics of capillary flow. *Physical Review*, 17(3), 273-283.
doi:10.1103/PhysRev.17.273

Yang, X. (2014). *Organic fillers in phenol formaldehyde wood-adhesives*. (Doctor of Philosophy), Virginia Tech, Blacksburg, VA.

Yang, X., & Frazier, C. (2016). Influence of organic fillers of surface tension of phenol-formaldehyde adhesives. *International Journal of Adhesion and Adhesives*, 66, 160-166.

Zheng, J., Fox, S. C., & Frazier, C. E. (2004). Rheological, wood penetration, and fracture performance studies of PF/pMDI hybrid resins. *Forest Products Journal*, 51(10), 74-81.

4. Influence of surfactant and fillers/extenders on Phenol-formaldehyde resin wetting and penetration

Abstract:

Veneer-based resins like phenol-formaldehyde are typically formulated with fillers and extenders to maximize the wetting behavior. However, it is unknown how the different components of the adhesive affect the wetting and resulting penetration. The wetting and penetration of phenol-formaldehyde base resin and derived adhesives were analyzed on three wood species. Wetting was analyzed with the sessile drop method, which observed the initial contact angle and change in contact angle over 35s; penetration was measured within each individual tracheid. The Lucas-Washburn equation was used to analyze the wetting and penetration by calculating the penetration and comparing it to the measured penetration. All contact angles were unfavorable because all adhesives formed a skin. Due to this skin formation, the Lucas-Washburn equation did not predict any penetration; however, the species and adhesive effects observed indicated favorable penetration. These findings did not suggest that the Lucas-Washburn equation was inadequate, but that the aqueous adhesive/wood system was too complex.

Keywords: Wetting, penetration, Lucas-Washburn equation, phenol-formaldehyde adhesive, wood-based composites

4.1 Introduction

Phenol-formaldehyde resins are formulated with fillers, extenders, and surfactants to aid in the wetting of wood for veneer based structural wood composites such as plywood (Bowyer et al., 2007). When formulated, the phenol-formaldehyde adhesive exhibits a shear thinning behavior; this high viscosity in the low shear region is typical for plywood applications. The shear thinning behavior is used to accelerate curing, yet allows the adhesive to retain the necessary flow properties (Bowyer et al., 2007). Little is known about how the different parts of the adhesive affect the wetting and penetration behavior. It is well-documented that bond performance is

directly related to adhesive wetting and subsequent penetration, but the quantitative relationship is unknown (Kamke & Lee, 2007).

Wetting is affected by liquid surface tension and solid surface energy (Berg, 2010); it is commonly defined as either favorable or unfavorable, if the contact angle is respectively less than or greater than 90°. Correspondingly, for porous substrates such as wood, the Young-Laplace relationship predicts that capillary uptake occurs when wetting is favorable; but not so when wetting is unfavorable (Berg, 2010). The Young-Laplace relationship does not account for liquid viscosity, but this is accounted for in the Lucas-Washburn equation (Lucas, 1918; Washburn, 1921), Equation 4-1, where the penetration distance, h , is related to the capillary radius, r , liquid surface tension, γ , liquid viscosity, η , cosine of the contact angle θ , and time, t .

$$h^2 = \frac{r\gamma \cos \theta}{2\eta} t \quad (4-1)$$

There have been many studies that predict adhesive or coating penetration based on the wetting behavior (Scheikl & Dunky, 1998; Shi & Gardner, 2001; Szekely et al., 1970), but few compare the actual penetration to the predicted penetration (de Meijer, Thurich, et al., 2001). The focus of this research was to improve understanding of adhesive wetting onto, and the subsequent penetration into, wood. This work only considers penetration due to capillary forces, the events prior to bond consolidation and compaction.

4.2 Materials and Methods

Materials

Phenol-formaldehyde, 14B346, a plywood resin (PLY RESIN), was supplied from Arclin Specialty Chemicals Inc. The PLY RESIN was additionally formulated with Modal™ alder bark (*Alnus rubra*) filler, wheat flour extender, sodium carbonate, 50% sodium hydroxide and water (PLY FORM), formulation shown in Table 4-1, materials provided by Willamette Valley Company. In addition, a surfactant, Sodium 2-ethylhexyl sulfate, obtained from Sigma-Aldrich, was added to PLY RESIN in two weight ratios based on the total resin mass, 1% and 0.5% (PLY SURF 1% and PLY SURF 0.5%). Three different wood species were obtained in the form of air-dried lumber: loblolly pine (*Pinus taeda*) from Critz, Virginia, USA; Douglas-fir (*Pseudotsuga*

menziesii) from Benton, Oregon, USA; and spotted gum (*Corymbia citriodora*) from Queensland, Australia. Specimens were rough-cut into ~9 mm³ cubes (attempting to obtain zero grain angle on the side grain surfaces), saturated in distilled water, and then microtomed (GSL1 sliding microtome) on the cross-sectional surface. The specimens were dried by cycling between vacuum (0.15 mmHg) and dry N₂ three times and then stored with dry N₂/molecular sieves. Specimens were equilibrated to ~6% moisture content in a desiccator over a saturated magnesium chloride solution.

Table 4-1: Phenol-formaldehyde formulation in mass fraction.

Formulation Content	Weight %
Water	18.4
PF Resin	22.8
Mix 30 s; 750 rpm	
Filler (Modal™ alder bark)	7.5
Add ~ 10 g/min; 750 rpm	
Extender (Wheat flour)	5.5
Add ~ 10 g/min; 750 rpm	
Sodium carbonate	0.5
Add ~ 10 g/min; 750 rpm	
Sodium hydroxide (50%)	3.0
Add ~ 1 min; 750 rpm	
Increase to 1200 rpm; mix 10 min	
PF Resin	42.3
Increase to 1500 rpm; mix 2 min	
Total Mixture	100.0

Resin viscosity

A TA Instruments AR G2 Rheometer was used (concentric cylinder, diameter = 30.35 mm, gap = 1 mm) to obtain steady-state flow curves (25°C; 0.5 to 3000 s⁻¹; ramping up in shear, then ramping down with no delay between ramps; steady-state criteria = 3 consecutive data points collected in 1 minute or less, shear stress ≤ 5% change).

Resin surface tension

Resin density was measured using a 10 mL graduated cylinder. Approximately one milliliter increments were added using a syringe and the density was obtained from the linear slope of the mass/volume plot; the corresponding correlation coefficients (R²) were always above 0.99.

Surface tensions were measured by the drop shape and drop weight methods at room temperature with a First Ten Angstroms, FTA 200, as described by Yang and Frazier (2016). The surface tensions reported below were from 10 observations analyzed separately using the drop shape and drop weight methods. The separate results from the two methods were not significantly different; the final value was averaged from the 10 observations, five from each method.

Wetting Measurements

Wetting measurements were conducted with the FTA200 equipped with the First Ten Angstroms environmental chamber. A VTI RH200 relative humidity generator was used to maintain ~30% relative humidity (using Ultrapure N₂) within the chamber in order to maintain the specimen moisture content at ~6%. The N₂ flowed into the chamber (500 mL/min) and was directed through open-cell foam in order to promote turbulent flow that would not deform the liquid droplet during video recording. A 1 μL resin droplet was placed in the middle of the specimen's cross-sectional surface. In most cases placement was restricted to earlywood regions, with exception of spotted gum, where no practical distinction was possible. The FTA200 camera was perpendicular to the specimen's longitudinal axis and tilted downwards (3°) to clearly observe the droplet in the middle of the specimen surface; light was reflected into the chamber to enhance image contrast. Using an adjustable stage, the specimen was raised up to "pluck" or transfer the droplet from the syringe tip to the specimen surface.

First Ten Angstroms FTA32 software was used to control video recording (acquisition rate: 1 image/10 seconds; initiated with a grey-scale pixel trigger), and to obtain contact angles averaged from both sides of the droplet. The video recording time (wetting period) was not fixed and was defined as the time from droplet deposition, through wetting, until the droplet was cured; this wetting period included an adjustment for specimen handling. To cure the resin, the specimen was microwaved for 2.5 minutes on 50% power. Ten replicates were obtained for each wood species/resin type.

Penetration Measurements

After the resin was cured, specimens were vacuum/pressure soaked in water and microtomed (GSL1 sliding microtome) to obtain 6-7 sections, 20-25 μm thick, nearest to the droplet center; sections were rinsed with DI water. Penetration was observed using a Nikon DS Fi-1 camera (Nikon Eclipse LV microscope) and length measurements were made using NIS BR Elements Software. A preliminary screening identified the section having the deepest resin penetration. Within that single section, the penetration within isolated tracheid cells (specific penetration) was measured, the average lumen diameter was obtained from 3 locations within each tracheid or fiber measured (13-71 cells per section). Within penetrated cells, the wetting favorability was judged from the appearance of the meniscus resulting after resin cure, discussed below.

Statistical Methods

Resin properties and wetting results were compared using a one-way ANOVA comparison and a Tukey's honestly significant difference (HSD) test for a pairwise comparison between each resin. The statistical analysis was run with a separation of species to determine what the most significant factors were for each species. The penetration data was not normal, therefore a log transformation was performed with the data, followed by an ANOVA and Tukey's HSD test.

4.3 Results and Discussion

Resin Properties

Table 4-2 shows the surface tension, viscosity and density measurements for all the resin and adhesive formulations studied (hereafter referred to as adhesives). All adhesives had significantly different surface tensions. The surface tension decreased with increasing surfactant, as observed

with PLY SURF 1% in Table 4-2. This is characteristic of the manufacturing environment, where surfactants are added to lower the surface tension of the adhesive for curtain coating applications. PLY FORM had a significantly higher viscosity than the other adhesives, and exhibited a lower surface tension when compared to the base resin, concurring with Yang and Frazier (2016). Both higher viscosity and lower surface tension can be attributed to the presence of fillers and extenders, therefore PLY FORM was expected to behave differently.

Table 4-2: Liquid properties of the four adhesives studied; average (stdev)

	Surface Tension (mN/m) (n = 10-16)	Viscosity (mPa·s) (n = 6-10)	Density (g/mL) (n = 3-4)
PLY RESIN	68.9 (0.6)	864.2 (72.3)	1.19 (0.0)
PLY SURF 0.5%	41.7 (0.9)	952.7 (86.3)	1.19 (0.0)
PLY SURF 1%	35.6 (0.7)	764.0 (88.7)	1.19 (0.0)
PLY FORM	52.2 (0.8)	2079.0 (499)	1.16 (0.0)

Wetting

Figure 4-1 shows typical wetting behaviors observed on loblolly pine cross-sectional surfaces (similar for Douglas-fir and spotted gum, not shown). Notice that the specimens appear to achieve an equilibrium contact angle; but only after an apparent increase in contact angle in the vicinity of 250 seconds. This anomalous behavior (and video recording not shown here) suggested that all adhesive droplets formed a skin during the measurements. The high molecular weight and the water-based nature of PLY RESIN was likely a contributing factor to the skin formation (Kamke & Lee, 2007; Marra, 1992). Consequently, it was grossly estimated that only the first 150 seconds of the data were useable. This was unfortunate because it prevented the use of a helpful wetting model (K-parameter) of Shi and Gardner (2001). Instead, wetting was evaluated using two parameters: the initial contact angle and the percentage change in contact angle over a period of 35 seconds.

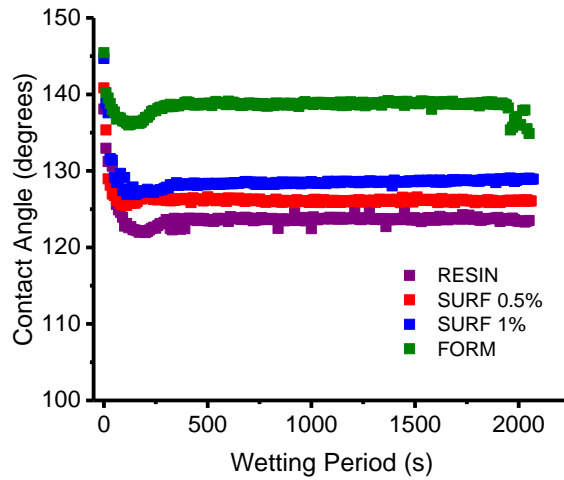


Figure 4-1: Example wetting of all adhesives studied on loblolly pine cross-sectional surfaces; note scale. (n = 10-11)

Effects from the adhesives and wetting behavior

Figure 4-2 summarizes the initial contact angles of all adhesives observed on the cross-sectional surfaces of all woods. All species exhibited unfavorable wetting (initial contact angle ≥ 90), and there was no effects from the adhesives. This was surprising since the surface tensions varied significantly in Table 4-2, indicating that the skin formation may have influenced the wetting behavior.

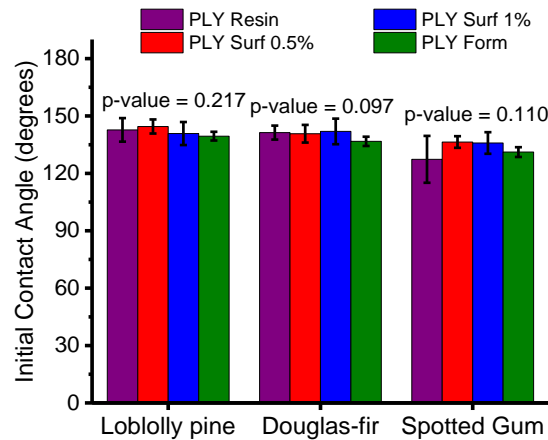


Figure 4-2: Initial contact angles of all adhesives as a function of species. Statistical significance shown by p-values, but only within each species. (n = 8-13)

Figure 4-3 summarizes the percentage change in contact angle (ΔCA) of all adhesives observed on the cross-sectional surfaces of all woods. Loblolly pine stood out as being the only species that exhibited adhesive effects. The only significant ΔCA was between PLY FORM and PLY SURF 0.5%, which can be attributed to the significantly higher viscosity of PLY FORM (Table 4-2). Since a higher surface energy indicates favorable wetting, the adhesive effects observed with loblolly pine could be attributed to the 39% greater surface energy of loblolly pine (Mirabile & Zink-Sharp, 2017). Mirabile’s findings do not explain the results, but help understand the complexities between the adhesive/wood wetting and penetration. It is also important to note that the magnitude of ΔCA with loblolly pine was not different from Douglas-fir and spotted gum, therefore the skin may have also affected the ΔCA results.

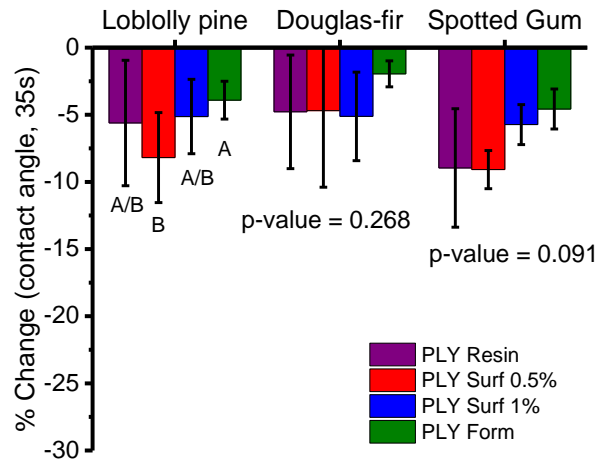


Figure 4-3: Percent change in contact angles of all adhesives as a function of species. Statistical significance shown by capital letters, but only within each species. (n = 8-13)

Penetration prediction via the Washburn equation

Specific penetration was defined as penetration depth measured within each isolated tracheid cell and was accompanied by lumen diameter measurements in three locations along the cell length, so as to enable penetration predictions. According to the Washburn equation, no penetration was expected since wetting was unfavorable (initial contact angle ≥ 90), Figure 4-2. However, Figure 4-1 was suspect because of the skin formation that could have altered the wetting behaviors.

Therefore, the Washburn predictions from the unfavorable contact angles were temporarily ignored, and the other parameters were investigated. Figures 4-2 and 4-3 show that both Douglas-fir and spotted gum had insignificant wetting behaviors among the adhesives. This indicates that penetration among the adhesives for Douglas-fir and spotted gum should be similar.

Figure 4-4 summarizes the penetration observed, even though penetration was not expected. There was an effect from the adhesives observed on all three species, however, no general trend was recognized. The penetration data was not normal, therefore a log transformation was performed with the data, and then an ANOVA and Tukey's HSD was performed to determine significant statistical differences.

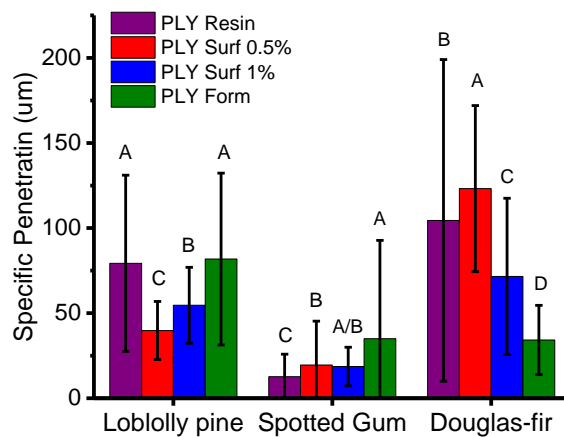


Figure 4-4: Specific penetration of all adhesives as a function of species. Statistical significance shown by capital letters, but only within each species. (n =13-66 cells per slide with n = 9-10 slides per species)

When comparing the penetration results to the resin properties in Table 4-2, the data seemed to have a surface tension and viscosity trend. Douglas-fir showed a viscosity trend, with significantly greater penetration observed with the low viscosity adhesives, compared to the significantly higher viscosity PLY FORM. With loblolly pine, penetration results implied a surface tension trend. A significantly greater penetration was observed with the significantly higher surface tension adhesives, PLY RESIN and PLY FORM, compared to the lower surface

tensions of PLY SURF 1% and 0.5%. Both of these agree with the Washburn equation (Eq. 4-1), that a higher surface tension and lower viscosity would increase penetration.

It is interesting to note that even though PLY FORM had the highest viscosity, it had significantly higher penetration with loblolly pine and spotted gum. This high viscosity, high penetration trend contradicts many findings (de Meijer, Thurich, et al., 2001; Gavrilović-Grmuša et al., 2010; Scheikl & Dunky, 1998). This could be due to the larger particles present in PLY FORM, which would not penetrate the cell walls, however the low penetration measured in Douglas-fir contradicts this theory. Figure 4-4 shows that the PLY FORM interactions are different, however, there was no clear explanation as to why.

Surfactants are added for curtain coating applications, but it is unknown how they affect the penetration. When comparing the two surfactant ratios, a significant difference in penetration was observed on both loblolly pine and Douglas-fir. However, the differences were opposite, with PLY SURF 1% having greater penetration on loblolly pine and PLY SURF 0.5% having greater penetration on Douglas-fir. This suggests that the minor change in amount of surfactant played a role in the penetration, however since the trends were opposite, further research is suggested. Since the surface tension, viscosity and surfactant trends were apparent but not consistent, further suggesting that the aqueous adhesive/wood system is complex.

Aside from the wetting behavior, the penetration was expected to be similar between Douglas-fir and loblolly pine for each resin since both have similar lumen diameters ($p = 0.555$). Figure 4-5 summarizes the specific penetration to observe species effects. As predicted, Douglas-fir and loblolly pine exhibited indistinguishable penetration with two of the four adhesives, PLY RESIN and PLY SURF 0.5%. With all four adhesives, spotted gum had significantly lower penetration than loblolly pine and Douglas-fir. Penetration in spotted gum was mostly in the fibers which have significantly smaller lumen diameter than the longitudinal tracheids in the two softwoods. Spotted gum is also known for the presence of tyloses in the vessels (Burch, 2015), which could limit penetration in the larger diameter vessel elements. Figure 4-5 indicates that the lumen diameter greatly impacted the penetration, in agreement with the Washburn equation (Eq. 4-1).

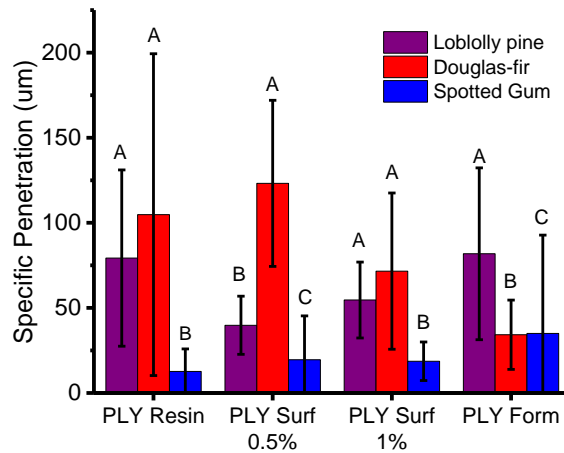


Figure 4-5: Specific penetration of all species as a function of adhesive type. Statistical significance shown by capital letters, but only within each adhesive type. (n =13-66 cells per slide with n = 9-10 slides per species)

Meniscus Favorability

The meniscus formed within each lumen wall was a result of cohesive and adhesive forces between the adhesive and lumen wall. When the adhesive forces were greater than the cohesive forces, the meniscus was semispherical concave. This indicates that the adhesive wicked up the lumen wall and penetration was favored, Figure 4-6. If the cohesive forces were greater than the adhesive forces, the convex meniscus was observed, indicating penetration was unfavored. Unfavorable penetration typically does not penetrate deep, as shown in Figure 4-6, unless pressure is added. Menisci favorability was judged within each tracheid or fiber cell (13-71 cells per section), and an average favorability was calculated for each section.

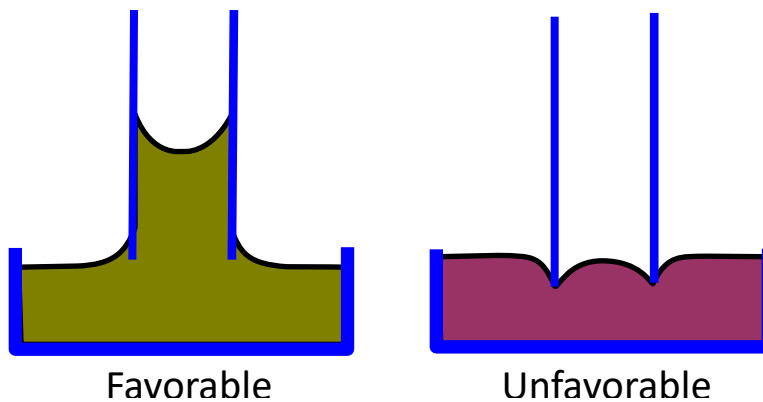


Figure 4-6: Diagrams showing the expected menisci under favorable and unfavorable wetting.

In reference to Figure 4-7, the average menisci was favorable for more than 50% of the tracheids; indicating that the adhesive penetration was favored for all systems. However, since all initial contact angles were unfavorable (Figure 4-2), something must have changed. Since these were water-based adhesives, water would have transferred into the cell wall increasing viscosity and decreasing surface tension; both suggest unfavorable penetration.

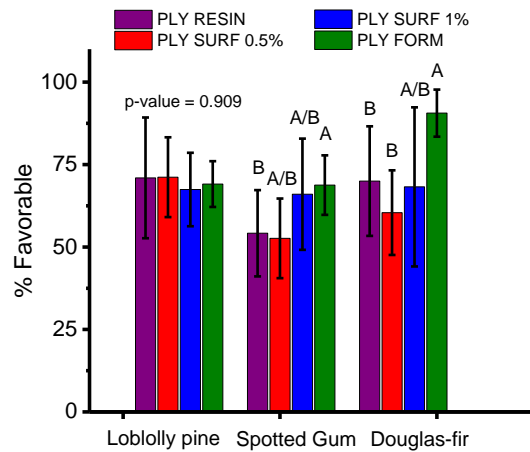


Figure 4-7: Average meniscus favorability of all adhesives as a function of species. Statistical significance shown by capital letters, but only within each species. (n =13-71 cells per slide with n = 9-10 slides per species)

As a parameter of the Washburn equation, time was not controlled, but it must be correctly measured to compare Washburn predictions with experimental measurements. This left the surface tension, viscosity and contact angle as factors that could have changed during the wetting process, influencing penetration. Since the contact angles were all unfavorable (greater than 90°), the Washburn equation predicted 0 μm of penetration, as mentioned previously. The skin observed affected the wetting observations, however it did not appear to affect penetration into the lumens, since the menisci were favorable.

Previous studies (de Meijer, Thurich, et al., 2001; de Meijer, van de Velde, et al., 2001) measured significantly less penetration with aqueous coatings than the Washburn equation

predicted. This was attributed to water transfer from the coating into the wood, however it was not noted whether the meniscus showed favorable penetration. The water absorption would significantly impact the adhesive properties. Surface tension was expected to decrease because of the decrease in polarity, due to water loss. At the same time, viscosity should increase as the solids content increased. The viscosity increase and surface tension decrease indicate that minimal penetration should be measured. However, it is possible that the surface tension could decrease enough to make the contact angle within the lumens (menisci) a positive value, favoring penetration. It is also important to note that the water being absorbed from the adhesive would be alkaline. It has been suggested that alkaline water absorption would increase the wood surface energy, which would also favor penetration (Wang et al., 2010).

Even though the Washburn equation did not predict penetration from the wetting, and favorable penetration was observed; it was proven that the aqueous adhesive/wood system changed throughout the wetting and penetration process. Since this change was not accounted for in the Washburn equation, the lack of penetration predicted was attributed to the complexity of the system studied.

4.4 Summary

Although it is known that wetting can impact penetration, few studies have actually compared wetting to penetration. The wetting and penetration of PLY RESIN and related adhesives were analyzed on three wood species. All initial contact angles were unfavorable and all adhesives formed a skin. Observations confirmed the hypothesis that PLY FORM would behave differently; however, it was not expected to exhibit greater penetration, as observed with loblolly pine and spotted gum. Observations also indicate that lumen diameter played a significant role in penetration. Due to the skin formation, the Washburn equation did not predict penetration, which contradicted the measured penetration. The results showed that favorable penetration occurred, and that the aqueous adhesive/wood system changed throughout the wetting and penetration process. Since these changes occurred and the Washburn equation was unable to account for them, it was concluded that this system was too complex for the Washburn equation to accurately predict penetration.

References

- Berg, J. C. (2010). *An Introduction to Interfaces and Colloids: The Bridge to Nanoscience*. Tuck Link, Singapore: World Scientific Publishing Co. Pte. Ltd.
- Bowyer, J. L., Shmulsky, R., & Haygreen, J. G. (2007). *Forest Products and Wood Science: An Introduction* (5 ed., pp. 353-382). Ames, Iowa: Blackwell Publishing.
- Burch, C. (2015). *Adhesion fundamentals of spotted gum (Corymbia citriodora)*. (Masters of Science Master's of Science), Virginia Tech, Blacksburg, VA.
- de Meijer, M., Thurich, K., & Militz, H. (2001). Quantitative measurements of capillary coating penetration in relation to wood and coating properties. *Holz als Roh- und Werkstoff*, 59, 35-45.
- de Meijer, M., van de Velde, B., & Militz, H. (2001). Rheological approach to the capillary penetration of coating into wood. *Journal of Coatings Technology*, 73(914), 39-51.
- Gavrilović-Grmuša, I., Dunky, M., Miljković, J., & Djiporović-Momčilović, M. (2010). Radial penetration of urea-formaldehyde adhesive resins into beech (*Fagus Moesiaca*). *Journal of Adhesion Science and Technology*, 24(8-10), 1753-1768. doi:10.1163/016942410x507812
- Kamke, F. A., & Lee, J. N. (2007). Adhesive penetration in wood- A review. *Wood and Fiber Science*, 39(2), 205-220.
- Lucas, R. (1918). Ueber das zeitgesetz des kapillaren aufstiegs von flüssigkeiten. *Kolloid-Zeitschrift*, 23, 15-22.
- Marra, A. A. (1992). *Technology of Wood Bonding Principles in Practice*. New York, NY: Van Nostrand Reinhold.
- Miracle, K. V., & Zink-Sharp, A. (2017). Fundamental bonding properties of Douglas-fir and southern yellow pine wood. *Forest Products Journal*, In-Press. doi:<https://doi.org/10.13073/FPJ-D-17-00019>
- Scheikl, M., & Dunky, M. (1998). Measurement of dynamic and static contact angles on wood for the determination of its surface tension and the penetration of liquids into the wood surface. *Holzforschung*, 52(1), 89-94.

Shi, S. Q., & Gardner, D., J. (2001). Dynamic adhesive wettability of wood. *Wood and Fiber Science*, 33(1), 58-68.

Szekely, J., Neumann, A. W., & Chuang, Y. K. (1970). Rate of capillary penetration and the applicability of the washburn equation. *Journal of Colloid and Interfacial Science*, 35(2), 273-278.

Wang, X., Huang, Z., Cooper, P., Wang, X.-M., Zhang, Y., & Casilla, R. (2010). The ability of wood to buffer highly acidic and alkaline adhesives. *Wood and Fiber Science*, 42(3), 398-405.

Washburn, E. W. (1921). The dynamics of capillary flow. *Physical Review*, 17(3), 273-283.
doi:10.1103/PhysRev.17.273

Yang, X., & Frazier, C. (2016). Influence of organic fillers of surface tension of phenol-formaldehyde adhesives. *International Journal of Adhesion and Adhesives*, 66, 160-166.

5. Summary and Future Research

The goal of this research was to improve the understanding between adhesive wetting onto wood, and the subsequent penetration into wood. This research specifically used the Lucas-Washburn equation to relate the wetting and penetration with aqueous adhesives and a non-aqueous resin on three different wood species. The Lucas-Washburn equation was originally designed for simple systems. In this research, the non-aqueous resin, pMDI, was the simplest system, and worked reasonably well with the Lucas-Washburn equation. The aqueous adhesive, PF PLY, was more complex, and the Washburn equation did not predict penetration.

When comparing pMDI wetting and penetration via the Washburn equation, the measured penetration was less than the calculated penetration. This was unexpected, but attributed to the Washburn equation calculations not accounting for the average tracheid length and the contact angle used in the Washburn penetration calculations was not correct. For the measured penetration, loblolly pine had greater penetration than Douglas-fir. This was shown to not be related to the average tracheid length, but to the greater surface energy of loblolly pine. The hypothesis, that the Washburn equation could predict pMDI penetration was supported. Further research is suggested to further understand the difference observed between the predicted and measured penetration, and to decide how to determine the best contact angle that should be used in the Lucas-Washburn calculations.

It is known that phenol-formaldehyde resins wet unfavorably, yet it had not been thoroughly studied to understand and relate wetting to penetration. When analyzing the influence of fillers and extenders on PF PLY resin wetting and penetration, the wetting behavior was difficult to observe due to the skin formation. This study found that even with unfavorable wetting, there was still penetration measured. It was concluded it was not the inadequacy of the Washburn equation prediction, but that the aqueous adhesive/wood system was too complex. In comparison to the non-aqueous pMDI, where wetting was favorable and there was dramatic penetration. The difference observed speaks to the concept of penetration, which is better? Deep penetration with little resin available at the surface for adhesion (pMDI), or minimal penetration with a large amount of resin available at the surface (PF PLY adhesives).

Clearly, the Lucas-Washburn was not accurate with the PF PLY systems, but the parameters in the equation changed throughout the process, causing this difference. Therefore, future work is suggested to use PF OSB instead. PF OSB was found to wet favorably from the wetting comparison section; if PF PLY which had unfavorable wetting, had favorable penetration it is probable that the PF OSB would have even more favorable penetration.

When simply comparing the wetting behavior, remarkable variation was observed between each system. The natural variation in wood can't be forgotten when considering the variation. Douglas-fir seemed to show changes from unfavorable to favorable wetting with PF OSB and UF. Among the aqueous resins, PF OSB and PF PLY exhibited unfavorable wetting with the exception of PF OSB on Douglas-fir. UF was favorable on loblolly pine and Douglas-fir, which could be due to the acid catalyst added to UF resin, decreasing the pH. The UF wetting was comparable to the favorable pMDI wetting on all three species. This similar behavior of the aqueous UF and non-aqueous pMDI speaks to the specific resin/wood interactions. UF should be studied more in depth, especially comparing the wetting and penetration.

6. APPENDICES

A. Applicability of the Lucas-Washburn equation for predicting pMDI penetration

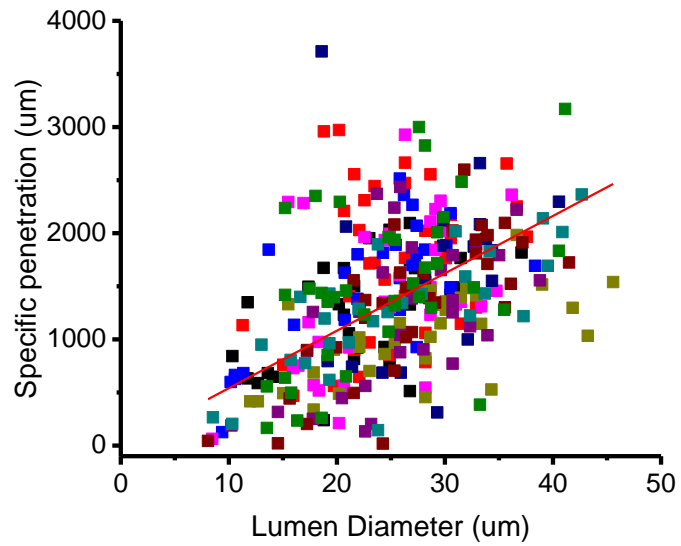


Figure 6-1: Correlation of specific penetration vs lumen diameter on Douglas-fir ($R^2 = 0.85$). (n =10)

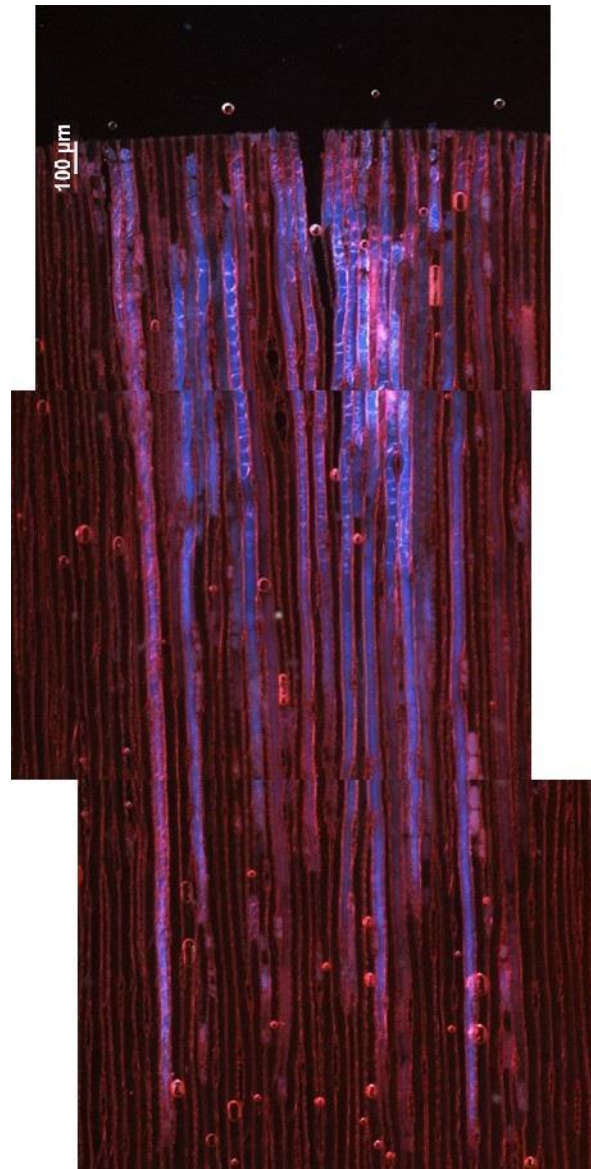


Figure 6-2: Example penetration of pMDI on loblolly pine; 5X (n =31-48 cells per slide with n = 10 slides)

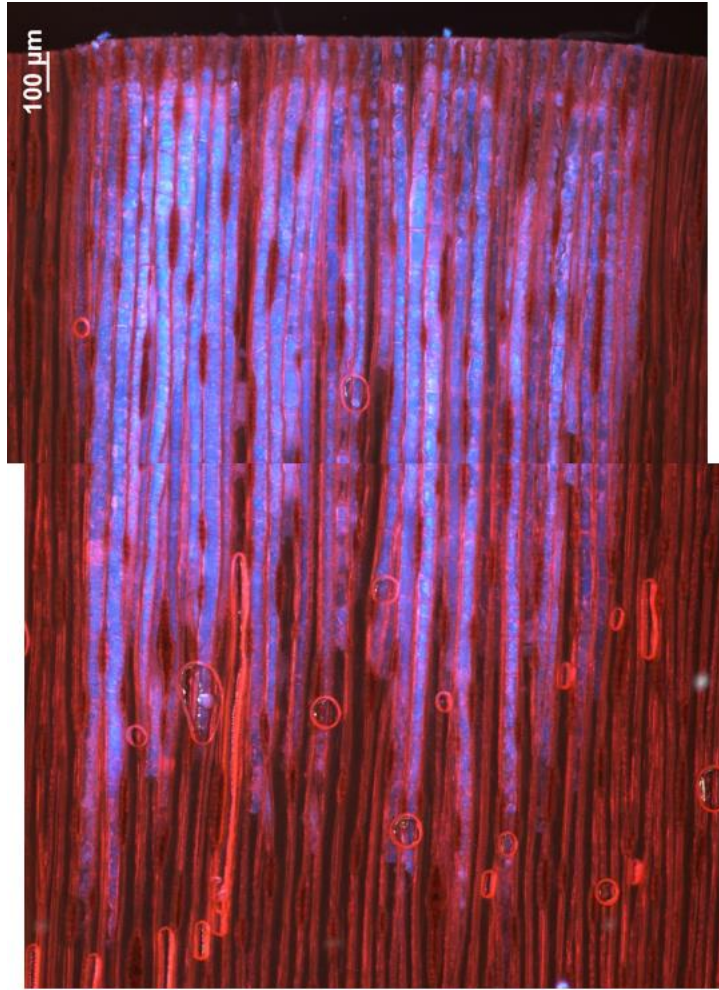


Figure 6-3: Example penetration of pMDI on Douglas-fir; 5X (n =18-39 cells per slide with n = 10 slides)

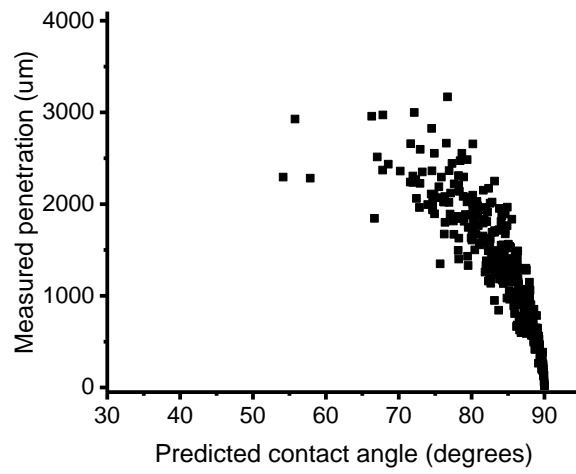


Figure 6-4: Calculated contact angle vs measured penetration on Douglas-fir. (n =10)

B. Influence of surfactant and fillers/extenders on Phenol-formaldehyde resin wetting and penetration

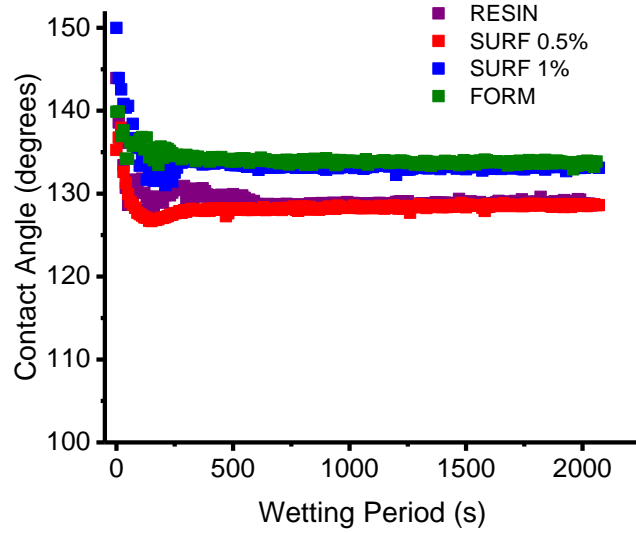


Figure 6-5: Example wetting curves of all adhesives on Douglas-fir cross-sectional surface, earlywood; note scale. (n = 9-13)

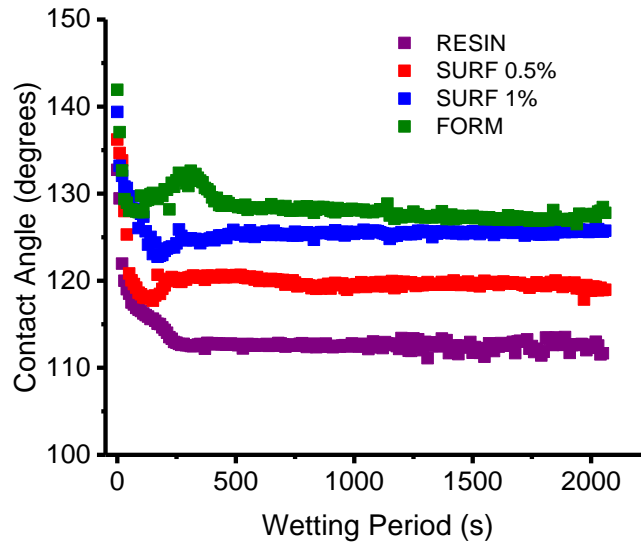


Figure 6-6: Example wetting curves of all adhesives on spotted gum cross-sectional surface; note scale. (n = 8-10)



Figure 6-7: Example penetration of PLY RESIN on loblolly pine; 5X (n =13-29 cells per slide with n = 10 slides)



Figure 6-8: Example penetration of PLY RESIN on loblolly pine; 5X (n =13-29 cells per slide with n = 10 slides)



Figure 6-9: Example penetration of PLY RESIN on loblolly pine; 5X (n =13-29 cells per slide with n = 10 slides)

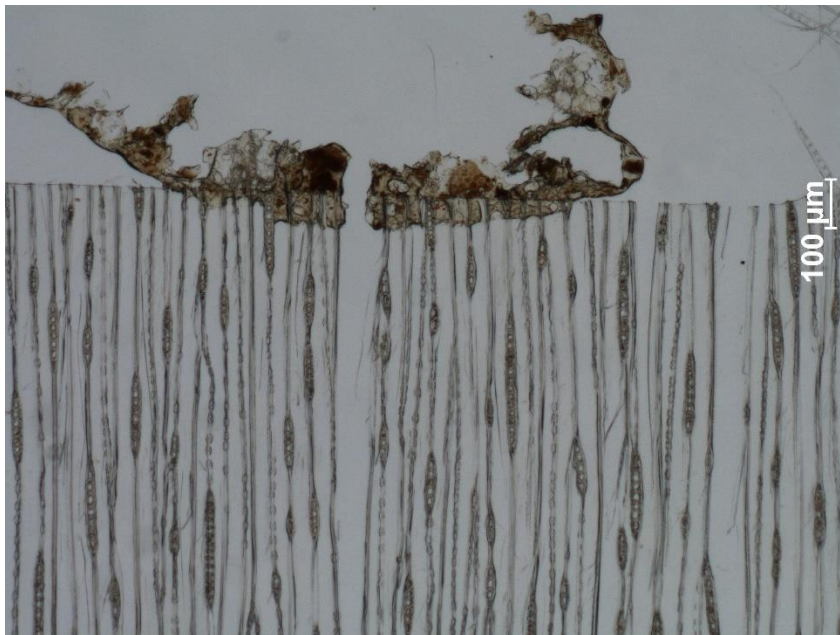


Figure 6-10: Example penetration of PLY FORM on Douglas-fir; 5X (n =16-24 cells per slide with n = 9 slides)

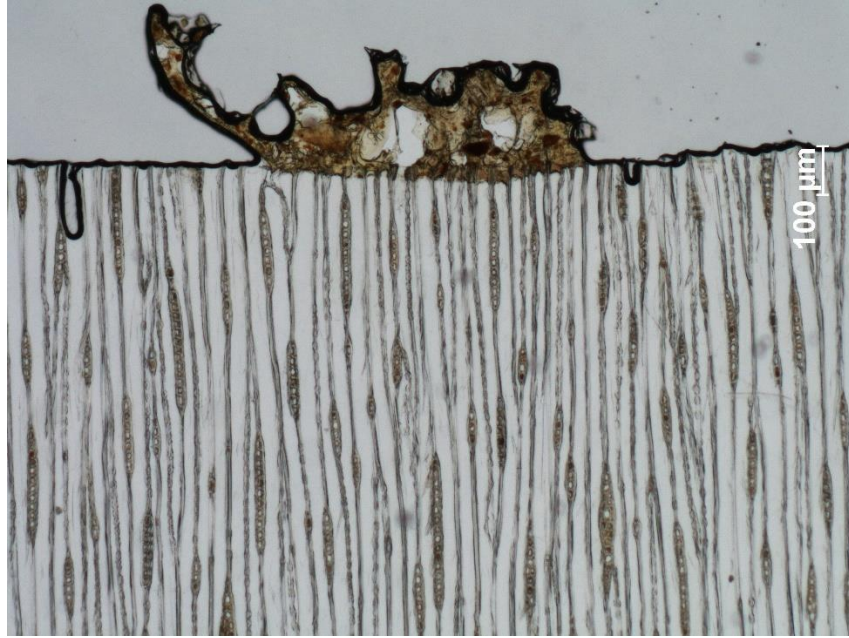


Figure 6-11: Example penetration of PLY FORM on Douglas-fir; 5X (n =16-24 cells per slide with n = 9 slides)



Figure 6-12: Example penetration of PLY FORM on Douglas-fir; 5X (n =16-24 cells per slide with n = 9 slides)



Figure 6-13: Example penetration of PLY SURF 0.5% on spotted gum; 10X (n =19-66 cells per slide with n = 10 slides)

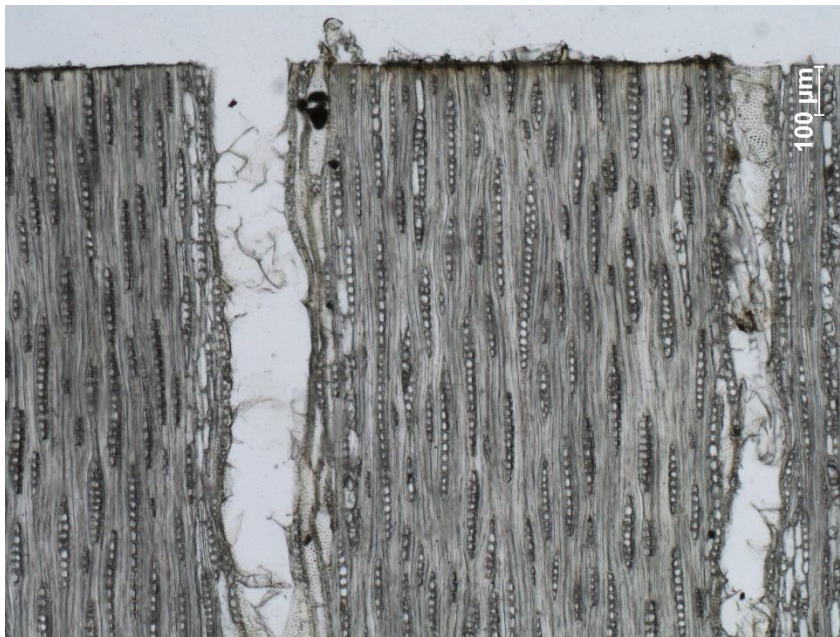


Figure 6-14: Example penetration of PLY SURF 0.5% on spotted gum; 10X (n =19-66 cells per slide with n = 10 slides)



Figure 6-15: Example penetration of PLY SURF 0.5% on spotted gum; 10X (n =19-66 cells per slide with n = 10 slides)

C. Viscosity Flow Curve

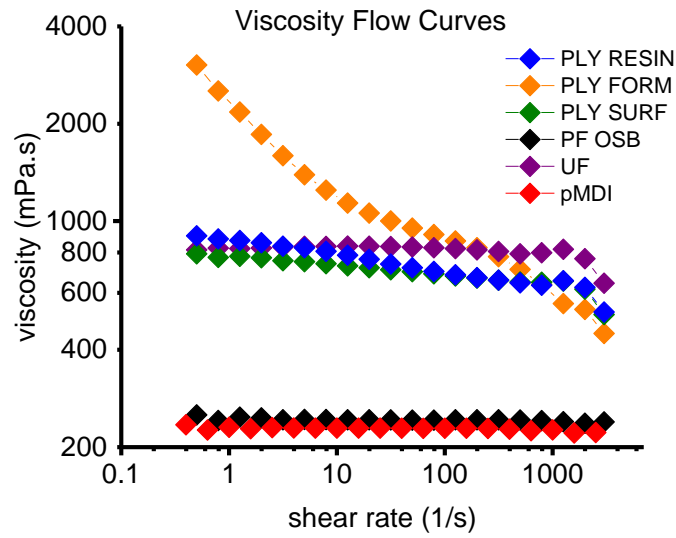


Figure 6-16: Viscosity steady-state flow curves (concentric cylinder; 0.5 to 3000 $\frac{1}{s}$; 25 °C) (n = 5-14)